A novel murine model of myeloproliferative disorders generated by overexpression of the transcription factor NF-E2

Kai B. Kaufmann,[1] Albert Gründer,[1] Tobias Hadlich,[1] Julius Wehrle,[1] Monika Gothwal,[1,5] Ruzhica Bogeska,[1,4,5] Thalia S. Seeger,[1] Sarah Kayser,[1] Kien-Binh Pham,[1] Jonas S. Jutzi,[1] Lucas Ganzenmüller,[1] Doris Steinemann,[8] Brigitte Schlegelberger,[8] Julia M. Wagner,[6] Manfred Jung,[6,7] Britta Will,[9,10] Ulrich Steidl,[9,10] Konrad Aumann,[2] Martin Werner,[2] Thomas Günther,[3] Roland Schüle,[3] Alessandro Rambaldi,[11] and Heike L. Pahl[1,4]

[1]Department of Experimental Anaesthesiology, Center for Clinical Research; [2]Institute of Pathology; and [3]Department of Urology; University Hospital Freiburg; and [4]Spemann Graduate School of Biology and Medicine, [5]Faculty of Biology, [6]Institute of Pharmaceutical Sciences, and [7]Freiburg Institute for Advanced Studies; Albert Ludwigs University Freiburg, 79085 Freiburg, Germany
[8]Institute of Cell and Molecular Pathology, Hannover Medical School, 30625 Hannover, Germany
[9]Department of Cell Biology and [10]Albert Einstein Cancer Center, Albert Einstein College of Medicine, Bronx, NY 10461
[11]Unità di Ematologia, Ospedali Riuniti Di Bergamo, 24128 Bergamo, Italy

The molecular pathophysiology of myeloproliferative neoplasms (MPNs) remains poorly understood. Based on the observation that the transcription factor NF-E2 is often overexpressed in MPN patients, independent of the presence of other molecular aberrations, we generated mice expressing an NF-E2 transgene in hematopoietic cells. These mice exhibit many features of MPNs, including thrombocytosis, leukocytosis, Epo-independent colony formation, characteristic bone marrow histology, expansion of stem and progenitor compartments, and spontaneous transformation to acute myeloid leukemia. The MPN phenotype is transplantable to secondary recipient mice. NF-E2 can alter histone modifications, and NF-E2 transgenic mice show hypoacetylation of histone H3. Treatment of mice with the histone deacetylase inhibitor (HDAC-I) vorinostat restored physiological levels of histone H3 acetylation, decreased NF-E2 expression, and normalized platelet numbers. Similarly, MPN patients treated with an HDAC-I exhibited a decrease in NF-E2 expression. These data establish a role for NF-E2 in the pathophysiology of MPNs and provide a molecular rationale for investigating epigenetic alterations as novel targets for rationally designed MPN therapies.

CORRESPONDENCE
Heike L. Pahl:
Heike.Pahl@
klinikum.uni-freiburg.de

Abbreviations used: AML, acute myeloid leukemia; ANC, absolute neutrophil count; ANOVA, analysis of variance; BFU-E, burst-forming units–erythroid; CBC, complete blood count; CGH, comparative genomic hybridization; CMP, common myeloid progenitor; ET, essential thrombocytosis; FISH, fluorescence in situ hybridization; GMP, granulocyte-monocyte precursor; HDAC, histone deacetylase; HDAC-I, HDAC inhibitor; hNF-E2, human NF-E2; HSC, hematopoietic stem cell; LT-HSC, long-term HSC; MEP, megakaryocyte erythroid progenitor; MLC, myosin light chain; mNF-E2, murine NF-E2; MPN, myeloproliferative neoplasm; mRNA, messenger RNA; NACE, naphthol AS-D chloroacetate esterase; PMF, primary myelofibrosis; PV, polycythemia vera; RDW, red cell distribution width; ST-HSC, short-term HSC; tg, transgenic.

The Philadelphia-negative myeloproliferative neoplasms (MPNs) constitute a group of closely related hematological disorders that includes polycythemia vera (PV), essential thrombocytosis (ET), and primary myelofibrosis (PMF) and share among other features a propensity to transform to acute leukemia. Despite recent advances attained through the discovery of a point mutation in the JAK2 kinase ($JAK2^{V617F}$) in a large fraction of MPN patients as well as various additional mutations in subgroups of MPN patients, the molecular etiology of these disorders remains incompletely understood.

Several lines of evidence support the hypothesis that aberrations preceding acquisition of the most common mutation, $JAK2^{V617F}$, contribute to the pathophysiology of these disorders. First, the malignant clone may extend beyond the cells that have acquired the $JAK2^{V617F}$

K.B. Kaufmann and A. Gründer contributed equally to this paper.

The Rockefeller University Press $30.00
J. Exp. Med. Vol. 209 No. 1 35-50
www.jem.org/cgi/doi/10.1084/jem.20110540

mutation (Kralovics et al., 2006; Nussenzveig et al., 2007). Second, in familial MPNs, the JAK2^{V617F} mutation does not constitute the predisposing allele, but rather is independently acquired by affected individuals (Cario et al., 2005; Jones et al., 2009). Third, after transformation of JAK2^{V617F}-positive MPNs, leukemic blasts often display chromosomal aberrations present in the chronic MPN phase but do not contain the mutant JAK2 allele (Campbell et al., 2006; Theocharides et al., 2007). This observation strongly suggests that the leukemic transformation occurred in a clonally expanded cell that had not incurred the JAK2^{V617F} mutation, hence in a pre-JAK2^{V617F} clone.

Interest in characterizing the primary MPN alterations is enhanced by recent data from clinical trials of several newly developed JAK2 inhibitors (Santos et al., 2010; Verstovsek et al., 2010). While ameliorating symptoms, counterintuitively in both JAK2^{V617F}-positive and -negative patients, these agents do not appear to alter disease burden or prevent leukemic transformation. Additional rationally designed therapies are clearly required for the treatment of MPN patients.

We have recently described overexpression of the transcription factor NF-E2 in patients with all three MPN subtypes, independent of the presence or absence of the JAK2^{V617F} mutation (Goerttler et al., 2005; Wang et al., 2010a). NF-E2 is expressed in hematopoietic stem cells (HSCs) as well as in the myeloid, erythroid, and megakaryocytic lineages and acts as an epigenetic transcriptional regulator and chromatin modifier (Andrews et al., 1993; Kiekhaefer et al., 2002; Onishi and Kiyama, 2003; Demers et al., 2007). At the β-globin locus, NF-E2 initiates chromatin remodeling and is required for the recruitment of both the MLL2 and the G9a histone methyltransferase complexes (Onishi and Kiyama, 2003; Demers et al., 2007; Chaturvedi et al., 2009). Likewise, NF-E2 recruits both histone acetyltransferases and histone deacetylases (HDACs), thereby modulating histone acetylation (Bulger et al., 2002; Brand et al., 2004). We have demonstrated that NF-E2 overexpression in HSCs ex vivo delays their erythroid and megakaryocytic maturation, causing the accumulation of excess numbers of mature progeny from a single HSC (Mutschler et al., 2009). To test the hypothesis that NF-E2 overexpression plays an integral role in the pathogenesis of MPNs in vivo, we have generated and characterized a novel murine model, a transgenic (tg) mouse overexpressing NF-E2 specifically in the hematopoietic lineages.

RESULTS

NF-E2 is overexpressed and functional in human NF-E2 (hNF-E2) tg mice

To explore the effect of NF-E2 overexpression observed in MPN patients in an in vivo model, we engineered tg mice expressing the hNF-E2 cDNA under control of the Vav promoter, which directs expression in all hematopoietic cells including the stem and progenitor compartments (Ogilvy et al., 1999). Overexpression of the hNF-E2 protein in murine BM was confirmed by Western blot (Fig. 1 A).

Two independent founder strains, termed 9 and 39, were obtained that display a median transgene expression threefold and 30-fold above the endogenous murine NF-E2 (mNF-E2) expression, respectively (Fig. 1 B). This precisely mirrors both the level of NF-E2 overexpression and the wide range in the degree of NF-E2 overexpression observed in patients with PV (Goerttler et al., 2005). NF-E2 transgene expression was also determined in defined, FACS-sorted precursor and stem cell populations. The human transgene was expressed in Ter119^{+}/CD71^{+} erythroid precursor cells (Fig. 1 C) as well as in long-term HSCs (LT-HSCs), short-term HSCs (ST-HSCs), common myeloid progenitors (CMPs), megakaryocyte erythroid progenitors (MEPs), and granulocyte-monocyte precursors (GMPs) of both strains (Fig. 1 D). hNF-E2 expression in these murine stem and progenitor cell compartments led to NF-E2 overexpression in LT-HSCs, ST-HSCs, and GMPs, similar to that observed in PV patients (Fig. 1 E). Contrary to what was observed in healthy human controls, endogenous mNF-E2 was not up-regulated physiologically in CMP and MEP cells (Fig. 1, D and E). Therefore, hNF-E2 transgene expression in murine CMPs and MEPs raises the level of NF-E2 in those cells to the high levels observed in their human counterparts. Collectively, NF-E2 tg mice display a degree and pattern of NF-E2 overexpression reminiscent of that observed in PV patients.

Interestingly, endogenous mNF-E2 levels were likewise elevated in hNF-E2 tg animals, most likely because of a positive feedback mechanism (Fig. 1 B; mNF-E2 expression [mean ± SEM]: WT, 1,954 ± 146; NF-E2 strain 9, 2,237 ± 90; NF-E2 strain 39, 2,663 ± 127; see also Fig. 10 B). In both strains, transgene integration occurred at a single genomic locus, as demonstrated by fluorescence in situ hybridization (FISH) analysis (Fig. 1 F). Higher levels of hNF-E2 expression in strain 39 were mediated by integration of multiple copies of the transgene at a single locus. Functional activity of the hNF-E2 transgene was confirmed by quantitating expression of β-globin, a well characterized NF-E2 target gene (Lu et al., 1994). In NF-E2 tg mice, β-globin expression was statistically significantly increased by a mean of 2.4-fold (Fig. 1 G), demonstrating that the NF-E2 transgene actively enhances expression of its physiological targets.

Peripheral blood phenotype of NF-E2 tg mice

NF-E2 tg mice developed thrombocytosis with an onset of 9 mo (Fig. 2 A). Correspondingly, the number of megakaryocytes in the BM was elevated in NF-E2 tg mice and increased further as the animals aged (Fig. 2 H). The age at clinical manifestation precisely reflects the epidemiology observed in patients with MPNs, who present in the sixth and seventh decade of life (Bilgrami and Greenberg, 1995).

Our murine model differs from MPN patients in that NF-E2 transgene expression is present from the outset in the hematopoietic system of tg mice, whereas the disease is acquired later in life in patients. We therefore investigated whether there is evidence of the acquisition of additional genetic aberrations in NF-E2 tg mice before the onset of

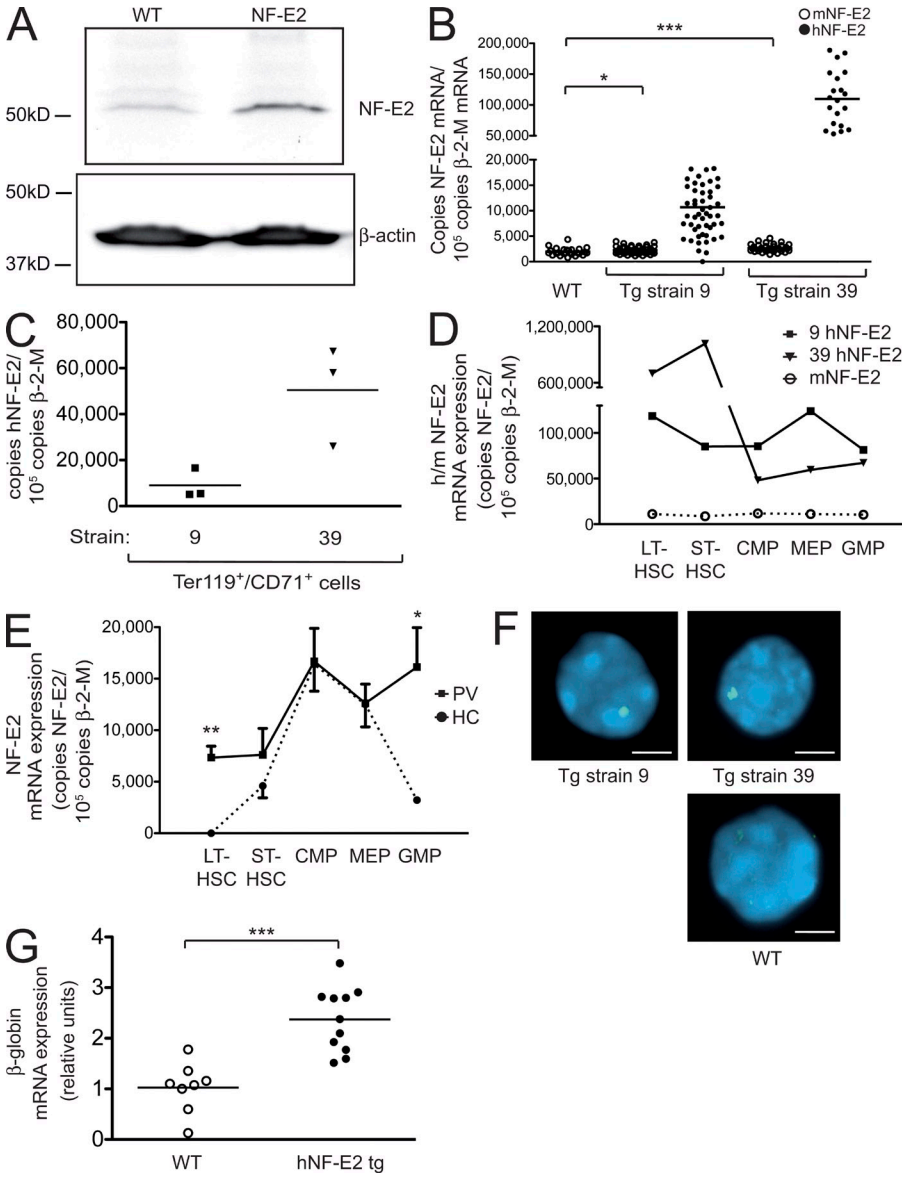

Figure 1. Construction and characterization of tg mice expressing hNF-E2. (A) Western Blot analysis of hNF-E2 expression in an hNF-E2 tg mouse (strain 39) and a WT littermate representative of $n = 4$ each. BM was harvested from animals of the indicated genotype, and total cell extracts were interrogated with an antibody that recognizes both human and mNF-E2. Equal loading was assured by reprobing with an antibody against β-actin. (B) Quantitation of murine and hNF-E2 expression in tg animals (both strain 9 and 39, as indicated; $n > 20$ each) and WT littermates. RNA was extracted from peripheral blood cells and assayed for murine and hNF-E2 expression by quantitative RT-PCR. Results are reported as copies of hNF-E2 or mNF-E2 expressed per 10^5 copies of the β-2-microglobulin housekeeping gene ($n > 20$ for each genotype). *, $P < 0.05$; ***, $P < 0.001$. (C) Transgene expression in erythroid cells. Ter119⁺/CD71⁺ double-positive erythroid progenitor cells were FACS sorted from peripheral blood of hNF-E2 tg animals ($n = 6$, three each from strain 9 and 39, respectively). RNA was isolated and assayed for hNF-E2 expression by quantitative RT-PCR. Results are reported as copies of hNF-E2 expressed per 10^5 copies of the β-2-microglobulin housekeeping gene. (D) Quantitation of murine and hNF-E2 expression in isolated stem and progenitor cells of tg animals. Defined stem and progenitor cell populations (LT-HSC, ST-HSC, CMP, MEP, and GMP) were FACS sorted from BM of hNF-E2 tg mice strain 9, strain 39, and WT littermate controls ($n = 2$ each) as described previously (Pronk et al., 2007), and human and mNF-E2 mRNA expression was measured by quantitative RT-PCR as detailed in B. Each animal was measured in duplicate, and averages are depicted. (E) NF-E2 expression in isolated stem and progenitor cells of PV patients and healthy controls. Defined stem and progenitor cell populations (LT-HSC, ST-HSC, CMP, MEP, and GMP) were FACS sorted from PV patients and healthy controls ($n = 3$ and 4, respectively) as described previously (Majeti et al., 2007; Will and Steidl, 2010), and NF-E2 mRNA expression was measured by quantitative RT-PCR as detailed in B. Mean and standard error of the mean are depicted. *, $P < 0.05$; **, $P < 0.01$. (F) FISH analysis of NF-E2 transgene integration. Peripheral blood smears of NF-E2 tg or WT mice ($n > 20$ for each strain) were probed by interphase FISH using the vav–hNF-E2 tg construct as a probe. For each sample, 100 cells were scored. Representative photographs showing single integration sites in both founder strains are depicted. Bars, 5 µm. (G) β-Globin mRNA expression. RNA was extracted from BM and assayed for murine β-globin mRNA expression and β-2-microglobulin housekeeping gene expression by quantitative RT-PCR. No difference was observed between mice of strains 9 and 39 ($n \geq 8$ each). Results are reported as relative expression levels using the ΔΔCt method and were analyzed for statistical significance using the Student's *t* test. ***, $P < 0.0001$. (B, C, and G) Horizontal lines indicate the mean.

thrombocythemia or during disease progression. Using high resolution array comparative genomic hybridization (CGH [array-CGH]), we compared NF-E2 tg mice with WT littermates at the ages of 6 mo ($n = 12$), before the onset of thrombocytosis, at 12 mo ($n = 12$), when thrombocytosis had developed, and at 18 mo ($n = 17$), when platelet counts were maximally increased. One mouse was reanalyzed at 20 mo, when platelet counts exceeded $2{,}500 \times 10^6$/µl (Fig. S1). Acquired genetic abnormalities were not visible in NF-E2 tg mice at any time point, nor was there evidence of clonal selection (Fig. S1 depicts five representative results from mice aged 18 mo and the one mouse aged 20 mo). Nonetheless, the long latency of disease development in our model implies the existence of cooperating events, perhaps point mutations.

The WBC count in NF-E2 tg mice was statistically significantly elevated (Fig. 2 B) and was accompanied by a rise in the absolute neutrophil count (ANC; Fig. 2 C). Correspondingly, neutrophilia is often observed in MPN patients

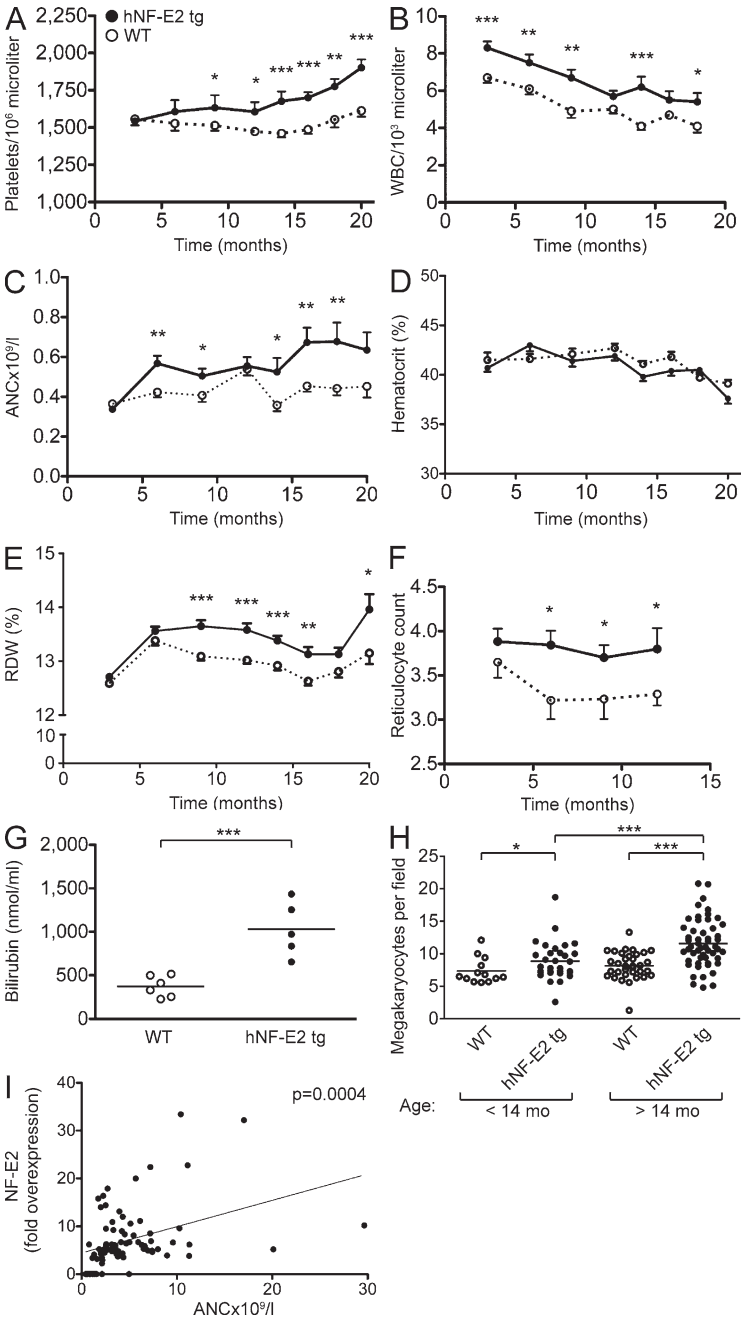

Figure 2. Hematological parameters of hNF-E2 tg and WT mice as well as correlation between NF-E2 expression and ANC in MPN patients. (A–G) Hematological parameters of mice. Peripheral blood was obtained by retroorbital puncture and analyzed on an Advia 120 system. For each time point, between 11 and 55 animals were analyzed. All data include mice of both tg strains, 9 and 39; no differences were observed between the two tg strains. Statistical analysis was conducted using a one-way ANOVA and a Bonferroni post-hoc multiple comparison test: *, $P < 0.05$; **, $P < 0.01$; ***, $P < 0.001$. Error bars indicate standard error of the mean. (A) Platelet counts. (B) WBC count. (C) ANC. (D) Hematocrit. (E) RDW. (F) Reticulocyte count. (G) Plasma serum bilirubin. (H) Number of megakaryocytes per visual field in BM sections of hNF-E2 tg mice and WT littermates. BM sections of hNF-E2 tg mice and WT littermates were stained with H&E, and megakaryocytes were identified morphologically. The number of megakaryocytes in 10 visual fields per mouse (100× magnification) was counted and is depicted stratified by age (n = 13, 31, 34, and 53 mice, respectively). Data include mice of both strains, 9 and 39; no differences were observed between the two tg strains. *, $P < 0.05$; ***, $P < 0.001$. (G and H) Horizontal lines indicate the mean. (I) ANC in MPN patients in relationship to NF-E2 mRNA expression (fold NF-E2 overexpression is defined as the fold increase over the mean of 50 healthy controls). ANC values of 80 MPN patients were obtained during routine follow-up. NF-E2 mRNA expression was determined in peripheral blood granulocytes of the same blood draw. The association was assessed using Spearman's correlation coefficient: $P = 0.0004$.

(Wehmeier et al., 1991). Interestingly, in a cohort of 80 MPN patients, the ANC correlated highly significantly ($P = 0.0004$) with the level of NF-E2 expression (Fig. 2 I). Somewhat surprisingly, in NF-E2 tg mice, the hematocrit remained within the normal range (Fig. 2 D). However, we observed a large increase in iron-containing histiocytes in the spleen (Fig. 3, A–D), indicating increased destruction of erythrocytes. In addition, both the reticulocyte count and serum bilirubin levels are elevated in NF-E2 tg mice, providing supportive evidence for increased red cell destruction (Fig. 2, F and G). Several genes encoding erythrocyte structural proteins are targets of NF-E2 (Boulanger et al., 2002; Steiner et al., 2009). Therefore, we propose that erythrocyte morphology is altered in NF-E2 tg mice, leading to increased destruction. Accordingly, in NF-E2 tg mice, the red cell distribution width (RDW), which provides a quantitative measure of red cell heterogeneity, was significantly elevated (Fig. 2 E). Patients with MPNs, especially PV, likewise often present with elevated RDW (anisocytosis; Li, 2002). The combination of thrombocytosis, WBC elevation, and normal hematocrit seen in the NF-E2 tg mouse model is frequently observed in both early PMF and in ET patients.

Stem and progenitor cell phenotype of NF-E2 tg mice

A pathognomonic feature of MPN patients is the growth of Epo-independent erythroid colonies, so called endogenous erythroid colonies (Prchal and Axelrad, 1974). We therefore examined the colony-forming potential of BM from NF-E2 tg animals and WT littermates. Contrary to human BM, WT murine BM already displays low levels of Epo-independent erythroid growth (Fig. 4 A). Overexpression of NF-E2 significantly increased Epo-independent growth of mature erythroid precursors (CFU-erythroid [CFU-E]; Fig. 4 A). Therefore, NF-E2 tg mice display a specific and diagnostic hallmark of MPN patients, Epo-independent erythroid colony formation. CFU-E growth in the presence of Epo is similar between the two genotypes (Fig. 4 A), whereas growth of more immature erythroid progenitors, so called burst-forming units–erythroid (BFU-E), is

physiologically independent of Epo and is likewise significantly elevated in NF-E2 tg mice (Fig. 4 B).

In addition to increased and Epo-independent erythroid colony-forming potential, NF-E2 tg mice contain significantly elevated numbers of granulocyte-macrophage precursors

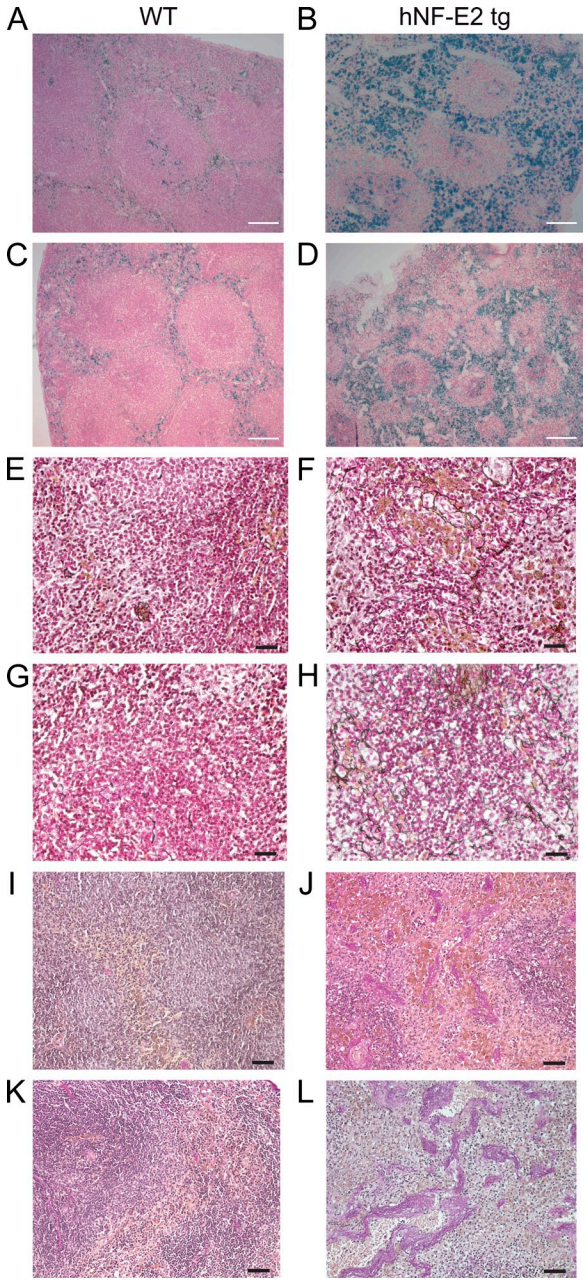

Figure 3. Histopathology of hNF-E2 tg mice. (A–D) Prussian blue staining of spleens of hNF-E2 tg mice (right) and control mice (left). Iron deposits stain blue. (E–H) Gomori's silver staining of spleens of hNF-E2 tg mice (right) and control mice (left). Reticulin fibers stain black. (I–L) Elastica van Gieson stain of spleens of hNF-E2 tg mice (right) and WT mice (left). Elastic fibers and nuclei stain black, collagen stains red, and smooth muscle stains yellow. The increase in iron deposits, fibrosis, and neovascularization was seen in mice of both tg strains, 9 and 39 ($n > 50$ each), to the same extent. Bars: (A–D) 100 µm; (E–H) 25 µm; (I–L) 50 µm.

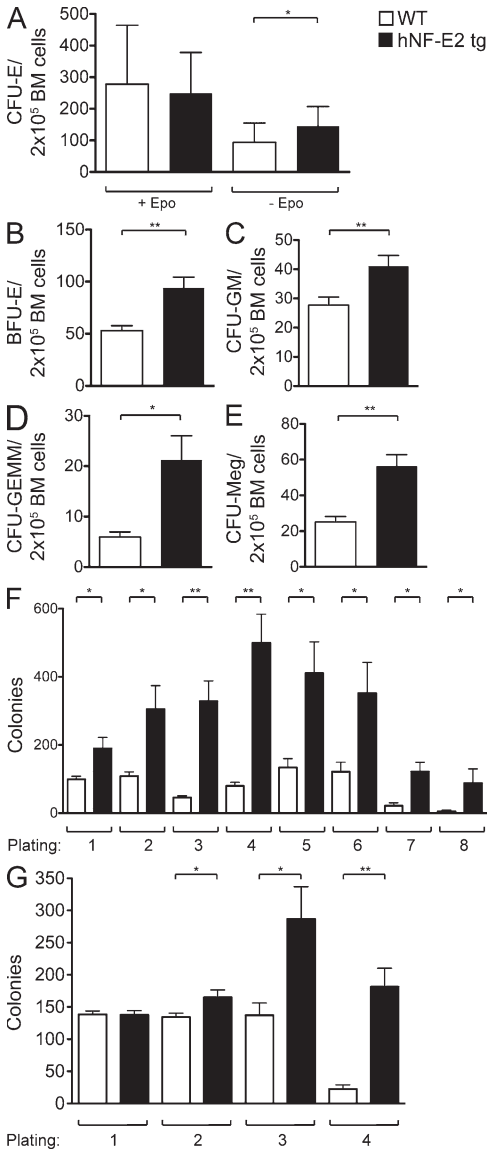

Figure 4. Hematopoietic progenitor cell enumeration and replating capacity in NF-E2 tg and control mice. (A–E) BM cells were seeded in methylcellulose (A–D) or collagen medium (E) to determine colony-forming potential. All data include mice of both tg strains, 9 and 39; no differences were observed between the two tg strains. Before scoring, methylcellulose dishes were stained with benzidine to allow identification of CFU-E and BFU-E. CFU-E were scored on day 4, and BFU-E, CFU-GM, and CFU-GEMM were scored on day 8. CFU-Meg were scored on day 12. Mean and standard deviation of at least 10 independent mice of each genotype are shown. (A) CFU-E. (B) BFU-E. (C) CFU-GM. (D) CFU-GEMM. (E) CFU-Meg. (F and G) Replating capacity of BM from hNF-E2 tg and WT littermates in the FVB/N background (both 9 and 39; $n = 4$ and 7, respectively; F) and the C57BL/6 backcrossed background ($n = 6$ each; G). BM cells were seeded in methylcellulose, and the number of colonies was scored after 8 d. Subsequently, the cells were harvested and subjected to a second round of colony growth. After 8 d, colonies were again scored and replated for a third time. In total, eight rounds of replating were performed in FVB/N mice (F) and four rounds in C57BL/6 mice (G). Error bars indicate standard error of the mean. *, $P < 0.05$; **, $P < 0.01$.

(CFU-GM; Fig. 4 C) and multipotent granulocyte-erythroid-macrophage and megakaryocyte precursors (CFU-GEMM; Fig. 4 D), as well as drastically elevated numbers of megakaryocyte precursors (CFU-Meg; Fig. 4 E). The observed increase in hematopoietic progenitors of all three myeloid lineages in NF-E2 tg mice corresponds well with the trilineage hyperplasia characteristic of MPN BM histology (Swerdlow et al., 2008).

Next, we examined whether NF-E2 tg BM cells display altered self-renewal capacity in serial replating assays. Although in our FVB/N strain WT control mice lost the capacity to form colonies after the sixth replating, NF-E2 tg mice retained the ability to form colonies beyond the seventh replating (Fig. 4 F). In addition, in every replating, NF-E2 tg mice formed statistically significantly more colonies than WT control mice. Enhanced colony formation and replating capacity was observed both with mice older than 12 mo, which were thrombocythemic, as well as with young mice, which did not yet show the platelet phenotype. Because there are very few published data on serial replating assays in FVB/N mice and WT mice in strains such as C57BL/6 do not show appreciable colony growth beyond the third replating, we backcrossed our NF-E2 tg FVB/N mice into a C57BL/6 background and used BM from C57BL/6 NF-E2 tg mice and WT littermate controls in serial replating assays as well (Fig. 4 G). As published (Huntly et al., 2004), WT C57BL/6 mice did not form large numbers of colonies after the third replating. In contrast, NF-E2 tg C57BL/6 mice retained the ability to form the initially high number of colonies into the fourth replating (Fig. 4 G). Therefore, NF-E2 tg mice display increased self-renewal capacity in two different genetic backgrounds.

We hypothesized that the pathophysiological changes observed in NF-E2 tg mice are the consequence of elevated NF-E2 activity in hematopoietic stem and progenitor cells. If this is true, the disease must be transferable to secondary mice by BM transplantation. BM from NF-E2 tg mice as well as from WT littermates (n = 5 each, which carry the CD45.1 allele) was therefore transplanted into lethally irradiated secondary FVB/N CD45.2$^+$ recipients (Guibal et al., 2009). Engraftment exceeded 95% donor cells in all mice. 8 wk after transplantation, complete blood counts (CBCs) were measured, and hematopoietic colony-forming potential was enumerated. As detailed in Fig. 5, secondary recipient mice engrafted with NF-E2 tg BM showed statistically significantly increased platelet numbers compared with mice engrafted with WT BM (Fig. 5 A), recapitulating the thrombocytosis observed in primary NF-E2 tg mice. Moreover, colony formation was significantly increased in NF-E2 tg recipients (Fig. 5 B). Specifically, as in the primary NF-E2 tg mice, Epo-independent CFU-E growth, a hallmark of MPN patients, was highly significantly increased (Fig. 5 C). In addition, the numbers of BFU-E, CFU-GM, and the most immature CFU-GEMM colonies were likewise significantly expanded in secondary recipients of NF-E2 tg BM (Fig. 5, D–F). These data demonstrate that the hematopoietic phenotype conferred by NF-E2 overexpression is transplantable to secondary mice.

As MPN BM is characteristically hypercellular, we enumerated the number of BM cells in our tg mice. NF-E2 overexpression caused a highly significant increase in BM cellularity (Fig. 6 A).

In addition to their potential for colony formation, hematopoietic stem and progenitor cells can be identified and classified by their expression of characteristic combinations of cell surface markers (Passegué et al., 2005).

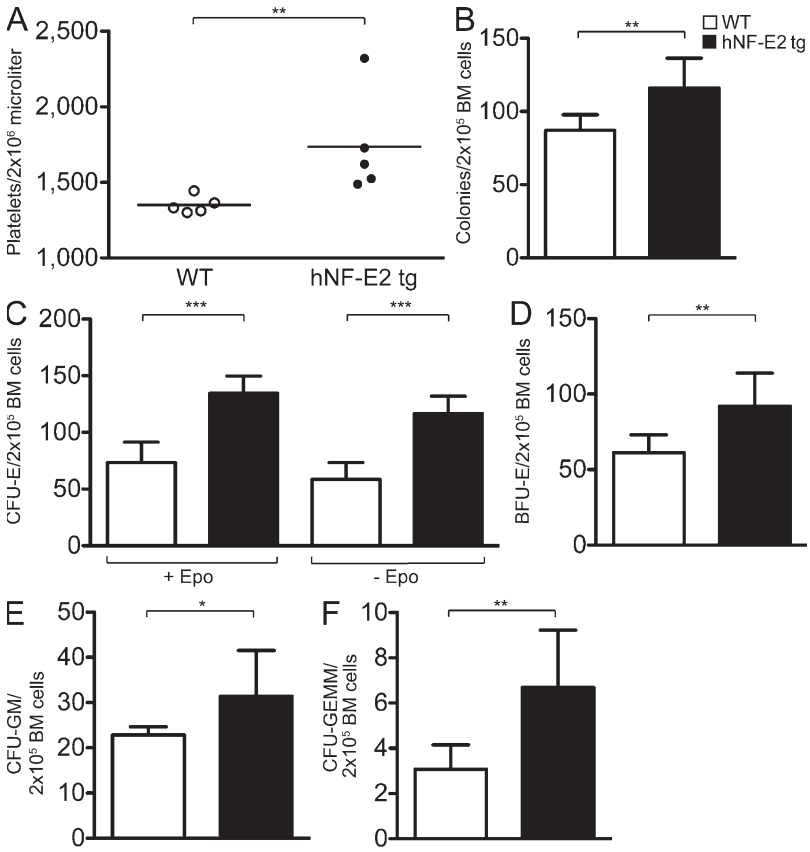

Figure 5. Platelet count and hematopoietic progenitor cell enumeration in secondary recipients of hNF-E2 tg and WT BM. (A) Platelet counts in secondary recipients of hNF-E2 tg or WT BM 8 wk after transplantation (n = 5 each). Horizontal lines indicate the mean. (B–F) BM cells of secondary recipients were seeded in methylcellulose to determine colony-forming potential. Before scoring, methylcellulose dishes were stained with benzidine to allow identification of CFU-E and BFU-E. CFU-E were scored on day 4, and BFU-E, CFU-GM, and CFU-GEMM were scored on day 8. Mean and standard deviation of six independently transplanted mice of each genotype are shown. (B) Total number of colonies. (C) CFU-E. (D) BFU-E. (E) CFU-GM. (F) CFU-GEMM. All data include donor mice of both strains, 9 and 39; no differences were observed between the two tg strains. *, $P < 0.05$; **, $P < 0.01$; ***, $P < 0.001$.

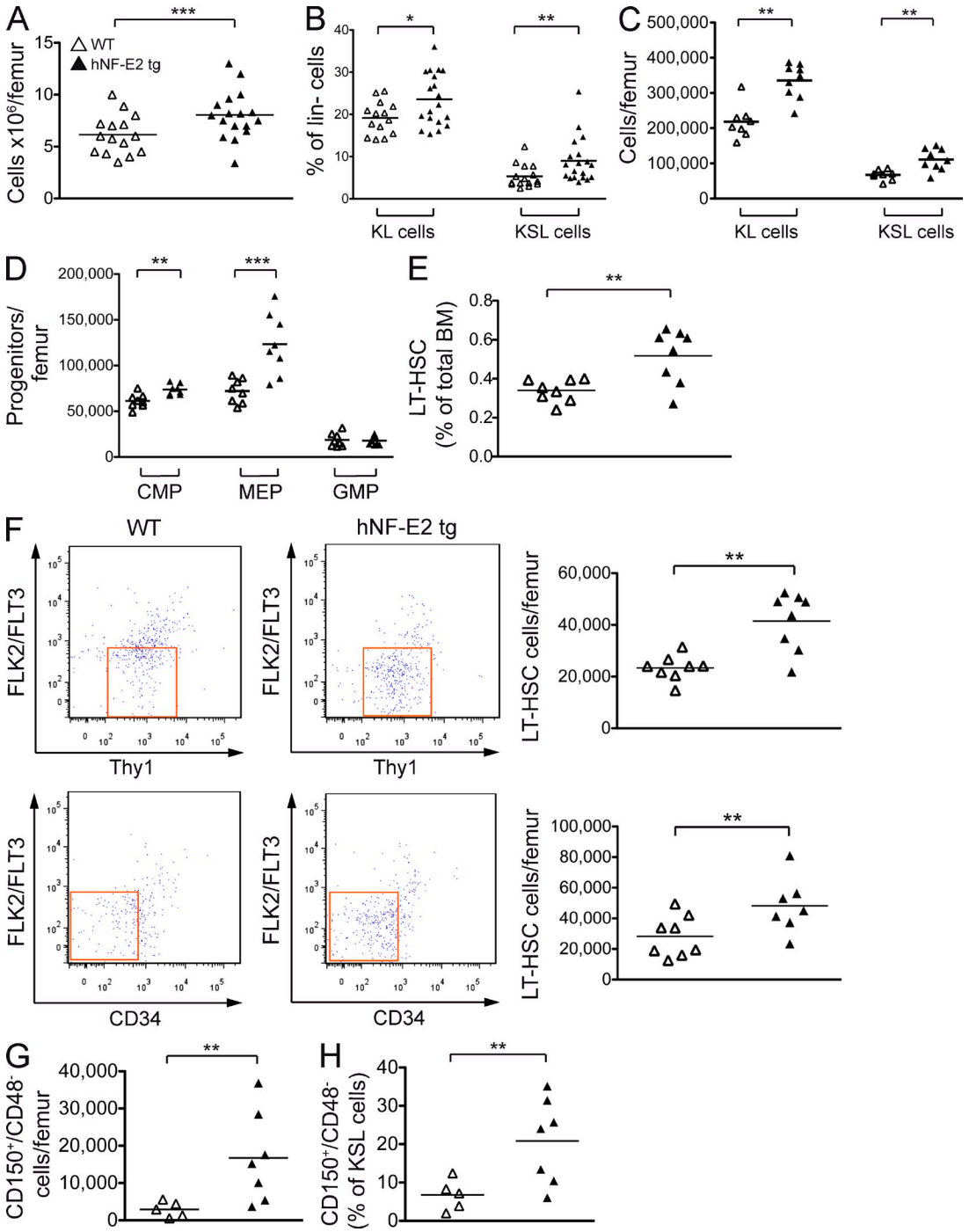

Figure 6. Hematopoietic stem and precursor populations in hNF–E2 tg and WT mice. (A) BM cells were harvested and enumerated; depicted is the number of cells per femur. (B–D) Cells were stained with antibodies against a cocktail of lineage markers as well as against c-kit, Sca-1, CD34, Fc-γR, Thy1.1, and Flt3/Flk2. (B) Lineage-negative, c-kit–positive, Sca-1–negative (KL) and lineage-negative, c-kit–positive, Sca-1–positive (KSL) cells are depicted as a percentage of lineage-negative cells. (C) The absolute number of KL and KSL cells per femur is depicted. (D) CMPs, MEPs, and GMPs were enumerated as previously described (Passegué et al., 2005), and the absolute number of cells per femur is depicted. (E and F) LT-HSCs were analyzed as previously described (Passegué et al., 2005). (E) LT-HSCs are depicted as a percentage of total BM. (F) The absolute number of LT-HSCs per femur is depicted. (G and H) Cells were stained with antibodies against a cocktail of lineage markers as well as against c-kit, Sca-1, CD150, and CD48. HSCs were analyzed as previously described (Kiel et al., 2005). (G) Absolute number of $CD150^+/CD48^-$ HSCs per femur. (H) Percentage of $CD150^+/CD48^-$ cells within the KSL (kit^+, $Sca\text{-}1^+$, lin^-) compartment. (A–H) All data include mice of both strains, 9 and 39; no differences were observed between the two tg strains (n = 5–17 per genotype, as indicated). Horizontal lines indicate the mean. *, $P < 0.05$; **, $P < 0.01$; ***, $P < 0.001$.

We therefore analyzed WT and tg BM cells by FACS. Both the percentage and the absolute number of the more immature KSL cells ($Kit^+/Sca^+/Lin^-$) and of the more mature KL cells ($Kit^+/Sca^-/Lin^-$) were increased by NF-E2 overexpression (Fig. 6, B and C). Therefore, the early hematopoietic stem and progenitor compartments are expanded in NF-E2 tg mice.

Within the KL compartment, both the CMPs and the MEPs were significantly elevated in NF-E2 tg mice (Fig. 6 D). Jamieson et al. (2006) have previously noted elevated numbers of CMPs in PV patients. Interestingly, within the KSL compartment, the absolute number and the percentage of the least mature long-term engrafting HSCs (LT-HSCs) were significantly elevated (Fig. 6, E and F). LT-HSCs can be characterized by two different sets of cell surface markers (Passegué et al., 2005). Applying either of these criteria demonstrates the increase in LT-HSCs in NF-E2 tg mice (Fig. 6 F). Similarly, when SLAM (signaling lymphocyte activation molecule) markers were used to define HSCs (Kiel et al., 2005), NF-E2 tg mice contained both a statistically increased number of $CD150^+/CD48^-$ cells per femur (Fig. 6 G) as well as an increased percentage of $CD150^+/CD48^-$ cells in the KSL compartment (Fig. 6 H). Jamieson et al. (2006) have reported elevated numbers of cells with an HSC phenotype in PV patients.

Morbidity and mortality of NF-E2 tg mice

Patients with MPNs experience a discrete but significant loss of life expectancy (Passamonti et al., 2004). NF-E2 tg mice likewise showed shorter survival (Fig. 7 A), displaying a loss of life expectancy of 8.8%, which is remarkably similar to that observed in PV patients (Passamonti et al., 2004). BM histology of NF-E2 tg mice revealed several characteristic features

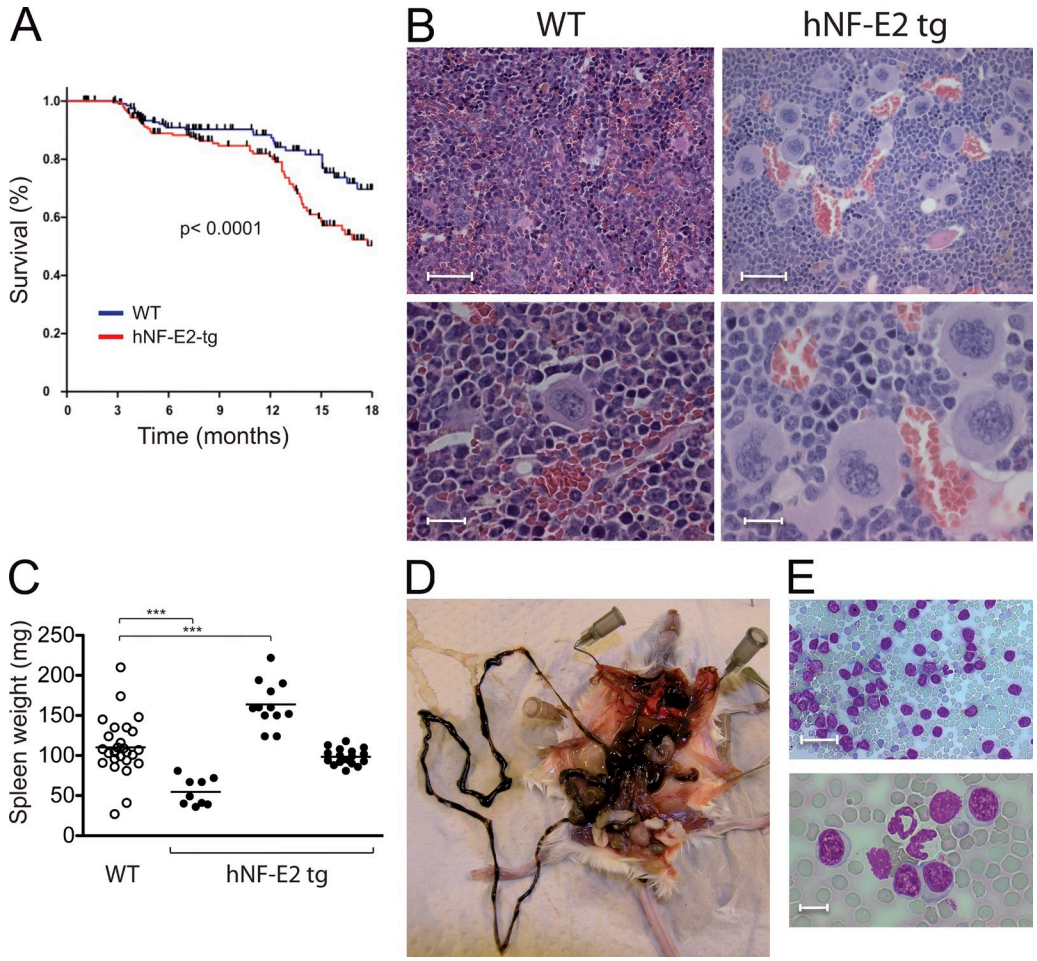

Figure 7. Disease progression and survival of hNF-E2 tg and WT mice. (A–E) All data include mice of both strains, 9 and 39; no differences were observed between the two tg strains. Representative data of $n \geq 30$ animals of each genotype are shown. (A) Kaplan Meyer analysis of survival of hNF-E2 tg and WT mice; $n > 50$ mice of each genotype were included. $P < 0.0001$. (B) Representative histology of WT and tg BM, H&E stain. (C) Spleen weights in WT and tg mice. NF-E2 tg mice were divided into three groups, representing weights ± 1 SD of the mean (80–120 mg), <1 SD of the mean (<80 mg), and >1 SD of the mean (>120 mg). Horizontal lines indicate the mean. ***, $P < 0.0001$. (D) Autopsy of an hNF-E2 tg mouse with gastrointestinal bleeding. (E) Peripheral blood smear of an hNF-E2 tg mouse that developed acute leukemia (WBC 86,000 cells/ml; blast counts: 33% in the peripheral blood, 44% in the BM, and 91% in the spleen; CBCs: Hct 29 [normal 40], Hb 10 [normal 14], platelet count 580 [normal in WT mice: 1,400], and a spleen weight of 863 mg, eight times normal). Bars: (B and E, top) 50 µm; (B and E, bottom) 10 µm.

of MPNs, including clustered, dysmorphic megakaryocytes (Fig. 7 B). NF-E2 tg mice frequently (25%; $n = 45$ animals) presented with splenomegaly, a characteristic finding in MPN patients. A subgroup of mice also showed small spleens of unclear etiology (Fig. 7 C). Similar to the presentation in MPN patients, reticulin fibrosis was observed (Fig. 3, E–H) in NF-E2 tg mice. In addition, NF-E2 tg mice showed increased vascularity (Fig. 3, I–L), a finding previously reported in MPN patients (Lundberg et al., 2000).

Tg mice frequently died abruptly of catastrophic gastrointestinal bleeding (Fig. 7 D). Strikingly, major hemorrhage is a leading cause of morbidity and mortality in MPN patients. At the age of 18 mo, 10% of the NF-E2 tg mice (of $n = 45$ mice analyzed) developed acute leukemia (Fig. 7 E). Blast counts ranged from 57–91%. Using the "Bethesda proposals for classification of nonlymphoid hematopoietic neoplasms in mice" published by Kogan et al. (2002), we classified the leukemic cells by histology (Fig. 8 A) and by immunofluorescence staining with antibodies against CD3, B220, and Ter119, as well as by naphthol AS-D chloroacetate esterase (NACE) staining (Fig. 8, B–D). Applying the Bethesda classification, we categorized the leukemias arising in NF-E2 tg mice, which were negative for CD3 and B220 (Fig. 8 B) and negative for Ter119 (Fig. 8 C), as well as for NACE (Fig. 8 D), as myeloid leukemias without maturation. Notably, 10–15% of PV and PMF patients transform to acute leukemia during follow-up (Cervantes et al., 2008).

Because the development of post-MPN acute myeloid leukemia (AML) is frequently accompanied by the acquisition of chromosomal aberrations (Groupe Français de Cytogénétique Hématologique, 1988), we investigated the leukemic mice for changes in chromosome integrity by array-CGH. In contrast to thrombocythemic mice, which showed no alterations by CGH analysis (Fig. S1), leukemic mice displayed multiple chromosomal abnormalities (Fig. 8 E). Consistent among all leukemias analyzed is a gain of genetic material on murine chromosome 15,

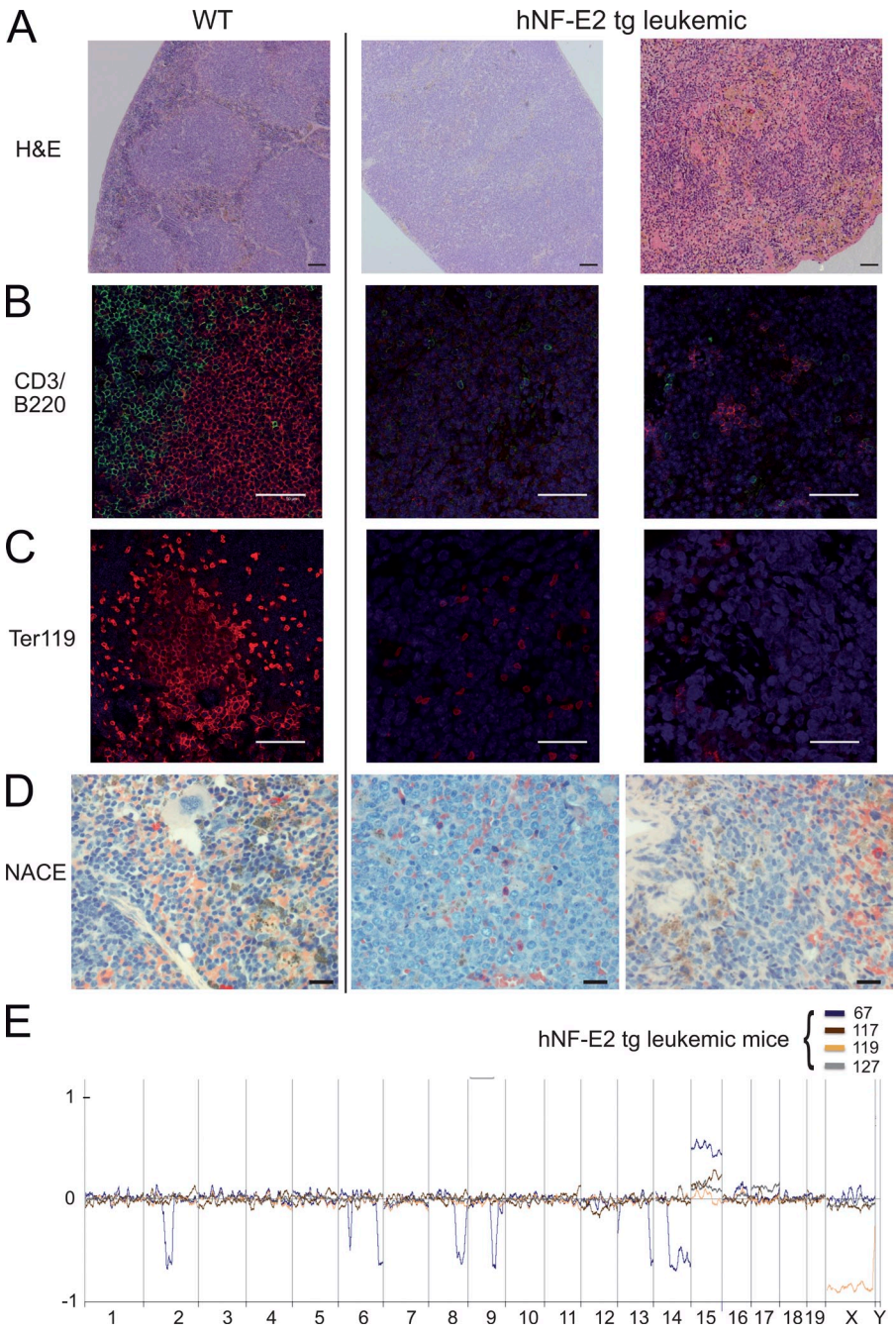

Figure 8. Phenotypic characterization of the leukemia arising in hNF-E2 tg mice. (A–D) Representative spleen histologies of WT mice (left) and NF-E2 tg mice with leukemic transformation (right). (A) H&E staining. (B) CD3 (green) and B220 (red) immunofluorescence staining. (C) Ter119 immunofluorescence staining. (D) NACE staining. NACE-positive cells stain red. Bars: (A) 100 µm; (B and C) 50 µm; (D) 20 µm. (E) Array-CGH of leukemic hNF-E2 tg mice and WT littermates. Genomic DNA of BM from individual leukemic hNF-E2 tg mice ($n = 4$, 1 from strain 9 and 3 from strain 39; identified by mouse number in the key) was hybridized to genomic DNA from a pool of $n = 10$ WT littermates. hNF-E2 tg genomic DNA was labeled with Cy3-dUTP, and WT DNA was stained with Cy5-dUTP. Detection of an equal amount of fluorescence in both DNAs results in a plot along the axis in the middle of the graph. Loss of DNA is depicted as signals below the axis, and gain of genetic material is depicted as signals above the axis.

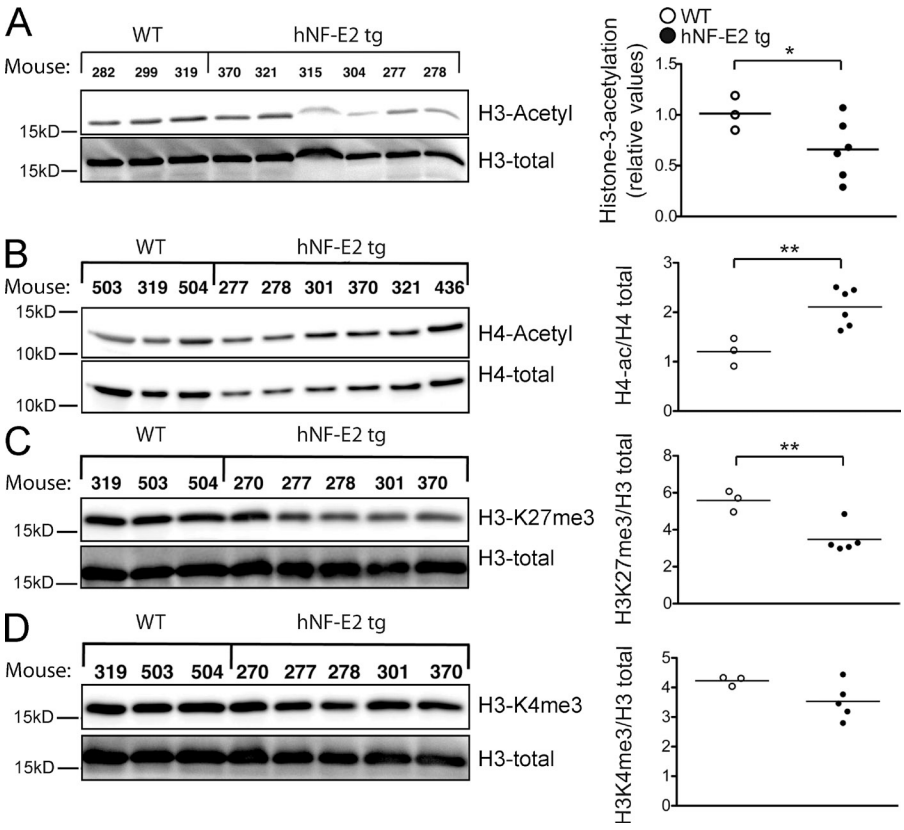

Figure 9. Chromatin modifications in hNF-E2 tg and WT mice. (A–D) Western blot analysis and densitometric quantification of histone H3 acetylation (A), histone H4 acetylation (B), H3K27me3 (C), and histone H3K4me3 (D) in BMs of WT and hNF-E2 tg mice (n = 3 and 6, respectively). 10 µg of protein was interrogated for the indicated modification of histone H3 or H4. The blot was stripped and reprobed with an antibody against total histone H3 or histone H4 to ensure equal loading. The ratio of modified histone H3 or H4 to total histone H3 or H4, respectively, was calculated for each animal. One untreated WT littermate was arbitrarily set at 100%, and all other animals were quantitated relative to this calibrator. All data include mice of both strains, 9 and 39; no differences were observed between the two tg strains. Horizontal lines indicate the mean. *, $P < 0.05$; **, $P < 0.01$.

which contains homologies to regions on human chromosomes 5p, 8q, 12q, and 22q. Interestingly, trisomy 8 is recurrently observed in both MPN and AML patients and has a poor prognostic impact in AML patients >60 yr of age and in secondary AML (Bench et al., 1998; van der Holt et al., 2007; Hussein et al., 2009; Koh et al., 2010).

HDAC inhibitor (HDAC-I) treatment of NF-E2 tg mice

Because of the documented role of NF-E2 in epigenetic regulation of gene expression, we examined the effect of NF-E2 overexpression on histone modifications. NF-E2 has been demonstrated to affect both histone methylation and histone acetylation (Kiekhaefer et al., 2002). In Western blot analysis, histone H3 acetylation was markedly decreased in NF-E2 tg mice (Fig. 9 A), whereas histone H4 acetylation was significantly increased, H3K27 trimethylation (H3K27me3) was significantly decreased, and H3K4me3 remained unaffected (Fig. 9, B–D).

In addition to this global histone analysis, we investigated histone modifications at specific sites within the β-globin locus, where the epigenetic effects of NF-E2 have been well documented (Demers et al., 2007). Consistent with the observed increase in β-globin expression (Fig. 1 G), we observed increases in histone H3K9 acetylation as well as in H3K4 dimethylation (H3K4me2) and H3K4me3 in NF-E2 tg mice at those sites within the β-globin locus previously demonstrated to be epigenetically modulated by NF-E2 binding (not depicted; Demers et al., 2007). These discrete changes are specific as the presence of histone H3K9 acetylation, H3K4me2, and H3K4me3 at two control sites, an inactive site within the β-globin locus (−9 kb), and a region of the myogenin promoter was unaffected and those sites showed equal occupation in NF-E2 tg mice and WT littermates (not depicted).

Because of the observed decrease in global histone H3 acetylation (Fig. 9 A), we treated NF-E2 tg mice with the HDAC-I vorinostat (SAHA) to restore physiological levels of histone H3 acetylation. Vorinostat treatment significantly increased H3 acetylation in NF-E2 tg animals (Fig. 10 A). Investigation of specific chromatin sites by chromatin immunoprecipitation quantitative PCR likewise demonstrated effective application of vorinostat, as histone H4 acetylation and histone H3 acetylation at the myogenin promoter, specifically H3K9 acetylation, increased significantly with treatment (not depicted). Consistent with the significant decrease in NF-E2 expression observed after vorinostat treatment (Fig. 10, B and C), a significant reduction in histone acetylation at exon 3 of the β-globin locus was seen (not depicted). The effect was less pronounced at the remaining sites in the β-globin locus.

Vorinostat treatment normalized the elevated mNF-E2 expression in NF-E2 tg mice, whereas it did not affect mNF-E2 expression in WT littermates (Fig. 10 B). In addition, vorinostat treatment reduced hNF-E2 expression (Fig. 10 C). We therefore examined whether vorinostat could also reverse the peripheral blood pathology observed in NF-E2 tg mice. After 11 d of vorinostat treatment, the previously elevated platelet counts of NF-E2 tg mice had normalized (Fig. 10 D). Platelet counts in WT mice also fell slightly but remained within the normal range. In contrast, the WBC counts were not significantly altered during vorinostat treatment in either genotype (not depicted). As expected,

the hematocrit fell during vorinostat treatment in both WT and tg mice, but this effect did not differ significantly between the two genotypes (not depicted). Spleen sizes were not affected by treatment with the HDAC-I (not depicted).

Phase I clinical trials of HDAC-Is in MPN patients have recently demonstrated efficacy of these drugs in controlling thrombocytosis and erythrocytosis (Rambaldi et al., 2010). We therefore sought to assess the effect of HDAC-I treatment on NF-E2 expression in MPN patients. NF-E2 messenger RNA (mRNA) expression was determined before treatment with the HDAC-I givinostat (ITF2357) and after 84 d of treatment. A statistically significant decrease in NF-E2 mRNA levels was observed in givinostat-treated patients (Fig. 10 E). At the same time, platelet counts decreased in these patients (Rambaldi et al., 2010). Normalization of NF-E2 levels by HDAC inhibition is therefore accompanied by a decrease in platelet numbers both in the murine model and in MPN patients.

DISCUSSION

After the discovery of mutations in the JAK2 kinase and the c-Mpl receptor in MPN patients, murine models carrying these alterations either by BM transplantation or by gene knockin have been created (Lacout et al., 2006; Pikman et al., 2006; Wernig et al., 2006; Akada et al., 2010; Li et al., 2010). These mouse strains recapitulate many pathophysiological changes observed in MPN patients, including erythrocytosis, thrombocytosis, leukocytosis, and Epo-independent erythroid colony growth.

Based on our observation that the transcription factor NF-E2 is overexpressed in MPN patients, we have engineered a novel murine model for MPNs. NF-E2 tg mice display many features of MPNs, including thrombocytosis, leukocytosis, characteristic MPN BM histology, and Epo-independent erythroid colony growth, as well as an expansion of the stem and progenitor cell compartments in the

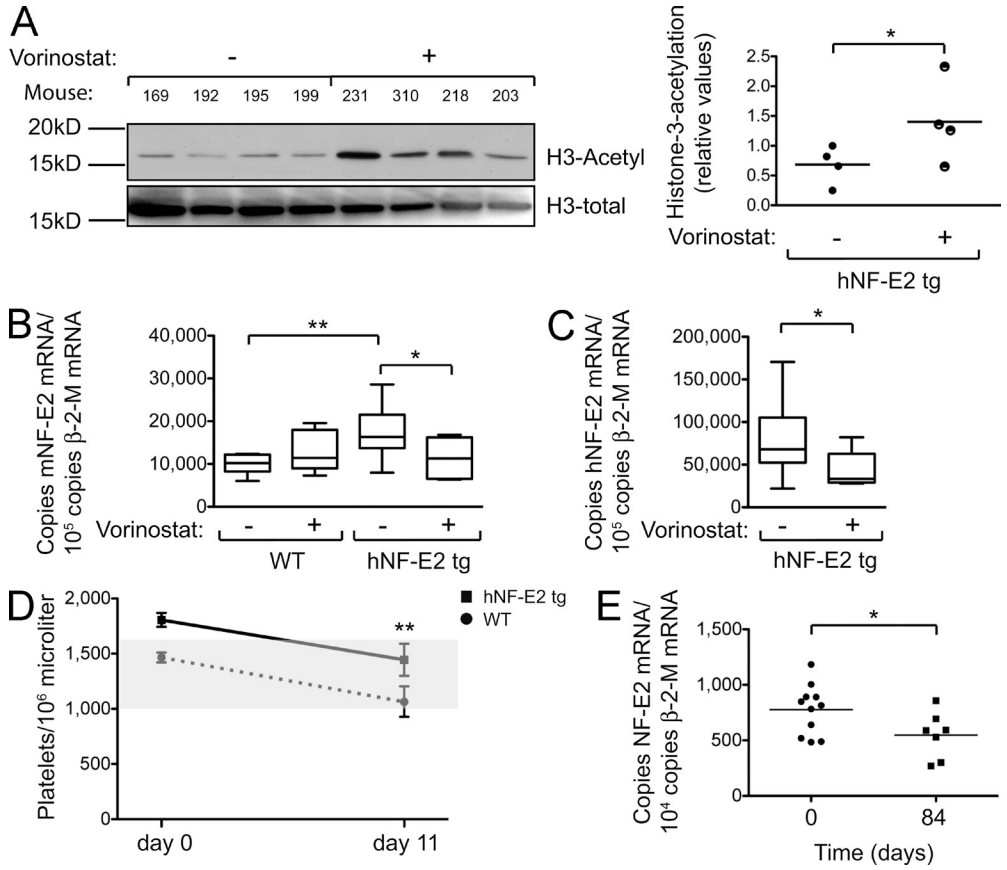

Figure 10. HDAC-I treatment of hNF-E2 tg and WT mice. (A) Western blot analysis of histone H3 acetylation in the spleen of untreated and vorinostat-treated hNF-E2 tg mice ($n = 4$ of each genotype). (B) mNF-E2 mRNA expression in untreated and vorinostat-treated WT and hNF-E2 tg mice ($n \geq 6$ for each group). See legend to Fig. 1 B for methods. Statistical analysis was conducted using a Student's t test: *, $P < 0.05$; **, $P < 0.01$. (C) hNF-E2 mRNA expression in untreated and vorinostat-treated hNF-E2 tg mice ($n \geq 6$ for each group). See legend to Fig. 1 B for methods. Statistical analysis was conducted using a Student's t test: *, $P < 0.05$. (B and C) Boxes show the 25th and 75th percentile, and the error bars show 1.5 times the interquartile range. (D) Platelet counts in untreated and vorinostat-treated WT and hNF-E2 tg mice at day 0 and 11 ($n > 5$ for each genotype). The shaded area indicates the normal range for this mouse strain. Statistical analysis was conducted using a one-way ANOVA and a Bonferroni post-hoc multiple comparison test: **, $P < 0.01$ for tg mice on day 11 versus day 0. Error bars indicate standard deviation of the mean. (E) NF-E2 mRNA expression in MPN patients before and after 84 d of treatment with the HDAC-I givinostat ($n = 11$ and 7, respectively; Rambaldi et al., 2010). For methods see legend to Fig. 1 B. (A and E) Horizontal lines indicate the mean. *, $P < 0.05$.

BM. In addition, however, NF-E2–overexpressing mice show two distinct features not observed in the JAK2- and c-Mpl–based MPN models.

First, NF-E2 tg mice frequently die of massive gastrointestinal bleeding. We suspect that the fibrosis observed in the spleens of NF-E2 tg mice (Fig. 3, E–H) may decrease tissue flexibility, which in combination with the pathological neovascularization (Fig. 3, I–L) coalesce to form this bleeding tendency. However, other etiologies are also possible.

Second and importantly, a proportion of NF-E2–overexpressing mice spontaneously develop AML. Both leukemic transformation and hemorrhage constitute major causes of morbidity and mortality in MPN patients. Interestingly, the recurrent genetic alteration observed in NF-E2 tg leukemic mice, a gain of genetic material corresponding to human chromosome 8, is also frequently observed in MPN patients and is associated with inferior survival and a higher rate of transformation to acute leukemia (Hussein et al., 2009). NF-E2 overexpression therefore constitutes a distinct molecular aberration observed in MPN patients that imparts an MPN phenotype in vivo, one that closely mirrors the severe complications affecting MPN patients.

The aforementioned data clearly argue that the aberrant NF-E2 expression observed in MPN patients constitutes a viable therapeutic target. In addition, our data argue that NF-E2, previously recognized to be important in erythroid and megakaryocytic maturation but known to be expressed in HSCs and mature granulocytes (Orlic et al., 1995; Toki et al., 2000), may contribute to the homeostasis of other lineages and compartments as well. Our observation that NF-E2 is overexpressed in very early stem cells (LT-HSCs) of both PV patients (Fig. 1 E) and our tg mice (Fig. 1 D) and the fact that expansion of the stem cell compartment is likewise observed in both patients and animal model supports this hypothesis.

Josefsson et al. (2011) have recently demonstrated that megakaryocytes must restrain their intrinsic apoptosis pathway and require the survival protein Bcl-$_{XL}$ for platelet shedding. Bcl-$_{XL}$ has been shown to be overexpressed in PV patients (Silva et al., 1998). Although there are no data implying NF-E2 in the regulation of Bcl-$_{XL}$ expression, it is possible that NF-E2 overexpression increases prosurvival signals in megakaryocytes. This could lead to the observed increase in megakaryocyte number in NF-E2 tg BM over the lifetime of the mouse (Fig. 2 H).

To date, transcription factor activities are difficult to influence pharmacologically. Therefore, it may be more feasible to counteract the effects of altered transcription factor activation. NF-E2 has been shown to alter chromatin structure and to modify histone marks, influencing both methylation and acetylation (Kiekhaefer et al., 2002). Although NF-E2 increases acetylation at the β-globin locus (Kiekhaefer et al., 2002), it also associates with HDACs. Specifically, in erythroid cells, NF-E2 has been shown to interact with BRAF35, a core member of the BRAF HDAC complex (Brand et al., 2004). We observed decreased histone H3 acetylation in NF-E2 tg mice. Interestingly, increased HDAC activity leading to decreased histone acetylation has been described in PMF patients (Wang et al., 2008).

Treatment of NF-E2 tg mice with the HDAC-I vorinostat restored physiological histone H3 acetylation and normalized the previously elevated platelet counts (Fig. 10, A and D). At the same time, NF-E2 expression decreased significantly (Fig. 10, B and C). We interpret these data with caution as HDAC inhibition has pleiotropic effects.

Several genes that play important roles in proplatelet formation are direct NF-E2 targets, such as the Rab GTPase RAB27b and the kinase adapter protein LIMS1/PINCH1 (Tiwari et al., 2003; Chen et al., 2007). Depletion of LIMS1/PINCH1 decreases the activity of Rac1, which regulates lamellipodium formation and cell spreading (Zhang et al., 2004). Proplatelet formation is regulated by a complex network of interactions in which the phosphorylation of myosin light chain (MLC) by MLC kinase plays a central role. MLC kinase activity, in turn, is regulated by Rho family proteins, especially Rac1 and Cdc42. Recently, Bishton et al. (2011) demonstrated that HDAC-Is cause an increase in phosphorylated MLC and reduced expression of the Rho family proteins RhoA, CDC42, and Rac1, thereby reducing proplatelet formation. In our model, increased NF-E2 activity may thus elevate levels of its target LIMS1/PINCH1, in turn increasing Rac1 activity. By increasing MLC phosphorylation and decreasing Rac1 activity, HDAC-Is will counteract these NF-E2 effects.

Matsuoka et al. (2007) have previously shown that treatment of erythroid cell lines with HDAC-Is decreases both NF-E2 and GATA-1 expression. GATA-1, in turn, is one of several regulators of NF-E2 expression (Moroni et al., 2000). It is therefore likely that one mechanism by which HDAC treatment lowers platelet levels is through decreasing NF-E2 expression. Suppression of physiological NF-E2 levels could therefore contribute to the observed thrombocytopenia in patients treated with HDAC-Is for other indications. In MPN patients, lowering of the supraphysiological NF-E2 levels can ameliorate thrombocytosis.

This model is also consistent with our data showing decreased NF-E2 expression in MPN patients treated with the HDAC-I givinostat (Fig. 10 E). Givinostat treatment showed clinical efficacy in MPN patients, inducing one complete and three partial responses in 13 ET/PV patients, accompanied by significant decreases in platelet counts. Major responses were also noted in 3/16 PMF patients treated (Rambaldi et al., 2010). Moreover, in preclinical models, the combination of DNA demethylation and HDAC inhibition corrected abnormal trafficking of PMF CD34$^+$ cells (Wang et al., 2009), decreased the clonogenicity of PMF but not normal cells (Shi et al., 2007), and increased apoptosis of PMF CD34$^+$ cells but did not affect healthy CD34$^+$ cells (Wang et al., 2010b).

Collectively, our data establish a role for aberrant expression of the transcription factor NF-E2 in the pathophysiology of MPNs. Moreover, they provide a strong molecular rationale for expanding the clinical investigation of HDAC-Is in

the treatment of MPN patients. In addition, they support the use of NF-E2 expression as a biomarker in correlative studies accompanying these clinical trials.

MATERIALS AND METHODS

Vector and transgene construction. The hNF-E2 cDNA was cloned into pCMX-PL2-3HA-10His to generate an HA–hNF-E2 fusion construct, which was subsequently expressed from the Vav promoter (Ogilvy et al., 1999). Linearized DNA, from which the plasmid sequences had been removed, was injected into FVB/N pronuclei. Presence of the transgene was determined by Southern blot analysis using the hNF-E2 cDNA as a probe and by PCR genotyping with primers located in the transgene construct and in exon 3 of the NF-E2 cDNA. All animal experiments were approved by the Regierungspräsidium Freiburg and complied with the regulatory standards of the animal ethics committee.

Western blotting and antibodies. Murine BM cells were lysed in 5× SDS buffer (250 mM Tris, pH 6.8, 10% SDS, 0.5% bromophenol blue, 50% glycerol, and 50 mM Dithio-DL-threitol) and subsequently sheared using a 26G needle. For analysis of acetyl histone H3, 10 mM sodium butyrate was added. Spleen extracts were obtained by lysis in SDS lysis buffer (62.5 mM Tris/HCl, pH 6.8, 2% SDS, 10% glycerol, 1 mM DTT, and 1× protease inhibitor cocktail [Roche]). The mixture was homogenized for 30 s and incubated for 15 min at 4°C, and cell debris was removed by centrifugation.

Cell lysates were subjected to SDS-PAGE and Western blotting. Primary antibodies against NF-E2 (Sigma-Aldrich), acetylated histone H3 (Millipore), anti-H3K4me3 (Active Motive), anti-H3K27me3 (Millipore), and anti-H4ac (Millipore) were used. The blots were stripped and reprobed for β-Actin (Sigma-Aldrich), total histone H3 (Abcam), or total histone H4 (Abcam) to control for equal loading. The immunocomplexes were detected using chemiluminescence Western blotting reagents (PerkinElmer). Densitometry analyses were performed using the Intas Laboratory Image 1D analysis software.

Quantitative RT-PCR. Quantitative RT-PCR experiments were performed using the following Assay on Demand (Applied Biosystems) products for gene expression analysis: hNF-E2 Assay on Demand mNF-E2: forward primer, 5′-CTTTCTGGTGCTTGTCTCACTGAC-3′; reverse primer, 5′-GGTGGCGTGAGTATACTTGAATTTG-3′; and probe, 6-FAM-ATCCAGAAAACCCC-MGBNFQ; murine β-globin Assay on Demand; and murine β-2-microglobulin Assay on Demand.

Reverse transcription of 400 ng of total blood or BM RNA was performed using the TaqMan Reverse Transcription kit (Applied Biosystems). Quantitative PCR assays were performed in duplicate in a PRISM 7000 Cycler (Applied Biosystems). A plasmid standard curve containing defined copy numbers was used to calculate gene expression as copy number per 100,000 copies of murine β-2-microglobulin mRNA.

Interphase FISH. Peripheral blood smears were dehydrated in an ethanol series (70, 90, and 100%, 3 min each) and subsequently air dried. Before FISH, the slides were treated with RNase followed by pepsin digestion as described previously (Ried et al., 1992). Interphase FISH was performed as previously described (Schempp et al., 1995). A biotinylated vav-promoter–NF-E2 cDNA (Fig. 1 A) was used as a probe and detected with FITC-conjugated avidin (Sigma-Aldrich). After FISH, the slides were counterstained with 0.14 µg/ml DAPI and mounted in Vectashield (Vector Laboratories). Preparations were evaluated using an epifluorescence microscope (Axiophot; Carl Zeiss).

CBCs. Peripheral blood was obtained retroorbitally using Na-heparin–coated capillary tubes (Hirschmann) and collected in heparin-coated tubes (Microvette CB300; Sarstedt). Blood counts were determined on an ADVIA120 hematology analyzer using the multispecies software (Bayer).

Phenotyping of leukemic mice. Peripheral blood smears were air dried and stained with May-Grünwald-Giemsa (Merck), and blast counts were determined by counting 20 visual fields of each animal. BMs and spleens of leukemic mice were analyzed histologically by Giemsa stain (Merck), and the blast count was determined by counting 20 visual fields. The leukemias were further characterized by immunofluorescence staining against CD3 (clone F7.2.38; Dako; used at 1:800; secondary antibody coupled to Alexa Fluor 488), B220 (clone RA3-6B2; BioLegend; used at 1:800; secondary antibody coupled to Alexa Fluor 546), and Ter119 (clone TER119; LifeSpan BioSciences; used at 1:800; secondary antibody coupled to Alexa Fluor 546) and counterstained with DAPI (Invitrogen). In addition, sections were stained for NACE.

Bilirubin measurements. Bilirubin levels were determined from retroorbitally drawn Li-heparin blood samples in a 1:250 dilution using a mouse total Bilirubin ELISA kit (Cusabio) according to the manufacturer's protocol.

Colony assays. BM cells were seeded in methylcellulose media with or without Epo (STEMCELL Technologies) for CFU-E assays or in media containing SCF, IL-3, and IL6, with or without EPO (STEMCELL Technologies) for BFU-E, CFU-GM, and CFU-GEMM colony growth and incubated for 4–8 d at 37°C, 5% CO_2. CFU-E colony growth was scored on day 4, and BFU-E, CFU-GM, and CFU-GEMM colony growth was scored on day 8. For correct identification of CFU-E and BFU-E, colonies were stained with benzidine. Megakaryocytic colonies were grown in chamber slides in Megacult C medium with collagen (STEMCELL Technologies) containing 10 ng/ml rmIL3 (PeproTech), 20 ng/ml rhIL6 (PeproTech), and 50 ng/ml rhTPO (PeproTech). Acetyl cholinesterase staining of mouse CFU-MK was performed according to the manufacturer's recommendations.

For serial replating, 3×10^4 BM cells were seeded in methylcellulose medium (STEMCELL Technologies), and colony growth was scored on day 8. Colonies were subsequently isolated from the methylcellulose by dilution in IMDM with 2% FCS (STEMCELL Technologies). Single cell suspensions were washed and reseeded at a density of 3×10^4/ml in methylcellulose medium, and colony growth was again scored on day 8. This process was repeated for up to eight replatings.

Secondary BM transplantation. 16 h before transplantation, recipient mice (FVB/N CD45.2$^+$; Guibal et al., 2009; a gift of D.G. Tenen [Harvard Medical School, Boston, MA] and S. Koschmieder [University Hospital Aachen, Aachen, Germany]) were irradiated twice with 4.5 Gy each at an interval of 4 h. BM was aspirated from NF-E2 tg donors or their WT littermates, resuspended in 15 µl of collagen matrix (Cell matrix; Nitta Gelatin Inc.), and injected into the BM cavity of the left femur using a 50-µl Hamilton syringe (705 RN) equipped with a 26G needle (RN Needle).

FACS analysis of hematopoietic stem and progenitor cells. BM was stained with a cocktail for lineage markers (CD3, CD11b, B220, Ter119, and Ly6G/6C; BioLegend), and lineage-negative cells (Lin$^-$) were analyzed for c-Kit (clone 2B8; eBioscience) and Sca-1 (clone D7; BioLegend) expression as described previously (Akashi et al., 2000; Christensen and Weissman, 2001; Passegué et al., 2003). Progenitor and stem cell subpopulations were identified as described previously (Akashi et al., 2000; Christensen and Weissman, 2001; Passegué et al., 2003) by staining with the following additional markers: CD34 (clone MEC14.7; BioLegend), Fc-γ-II/III-R (clone 93; eBioscience), Thy1.1 (clone OX7; BioLegend), and Flt3 (clone A2F10; eBioscience), CD48 (clone HM48.1; BioLegend), and CD150 (clone TC15-12F12.2; BioLegend). Positively staining cells as well as negative cells were determined by fluorescence minus one stainings, as depicted in Fig. S2 (B, D, and F). The gating strategies used are depicted in Fig. S2 (A, C, and E). For FACS sorting of populations to determine NF-E2 transgene expression, antibodies against Ter119 (clone TER119; ImmunoTools) and CD71 (clone R17217; Leinco) were used in addition.

MPN patients and healthy controls. Isolation of stem and progenitor cells from PV patients and healthy controls was performed as described previously (Will and Steidl, 2010). Peripheral blood samples were obtained from therapeutic phlebotomies of PV patients fulfilling the WHO criteria for diagnosis

(Swerdlow et al., 2008). Additional samples were obtained from the Tissue Bank of the Myeloproliferative Disease Research Consortium, which uses the same diagnostic criteria. Buffy coats of healthy volunteer blood donors were obtained from the University Hospital Freiburg Center for Blood Transfusion. The study protocol was approved by the local ethics committee of the University Hospital Freiburg, and informed consent was obtained from all patients in accordance with the Declaration of Helsinki.

Array-CGH. Array-CGH using high resolution 60-mer oligonucleotide arrays, with a median probe spacing of 10 kb (4 × 180k Mouse Genome CGH microarray; Agilent Technologies), was performed as previously described (Steinemann et al., 2008). In brief, 0.75 µg BM genomic DNA was labeled directly by random priming: test DNA (individual NF-E2 tg mice) with Cy3-dUTP and reference DNA (pool of 10 WT mice) with Cy5-dUTP. Slides were detected immediately after hybridization on a scanner (G2505B; Agilent Technologies) at a 2-µm resolution. Images were analyzed with the Feature Extraction Software, and the data were processed using the DNA-Workbench CGH analysis software (both from Agilent Technologies). The aberration algorithm ADM2 was applied, aberration filters were set to a threshold of 4.0, and at least five probes with mean $\log_2$ ratio of −0.6 were required.

Chromatin immunoprecipitation. Murine BM was harvested, depleted of erythrocytes by hypotonic lysis, and cross-linked in 1% formaldehyde for 10 min at room temperature. The reaction was quenched with 0.125 M glycine. After cell lysis in 50 mM Tris, pH 8.0, 1% SDS, 10 mM EDTA, 10 mM sodium butyrate, and protease inhibitors, the chromatin was sheared by sonication in a Bioruptor (Diagenode). The samples were diluted five times with 1% Triton, 20 mM Tris, pH 8.0, 150 mM NaCl, 0.01% SDS, 2 mM EDTA, 10 mM sodium butyrate, and protease inhibitors (Complete; Roche). After preclearing with Protein A agarose (Millipore), samples were incubated overnight with the primary antibody. Antibody–chromatin complexes were precipitated with protein A agarose and decross-linked, and the DNA was recovered by phenol/chloroform extraction. DNA representing sites within the β-globin locus was quantitated as previously described (Demers et al., 2007) using a standard curve generated from dilutions of chromatin and is reported as a percentage of the input fraction normalized to either an IgG or a total H3 control. Primers used were described in detail in Demers et al. (2007) and include the hypersensitive site 2 (HS2) at bp −3321, a site at bp −8913 to −8832 from the promoter (−9 kb), bp −69 to 11 of the promoter region (prom), bp 370–421 of exon 2 (Exon2), and bp 1289–1357 of exon 3 (Exon3) as well as bp −140 to −80 of the murine myogenin promoter. The following antibodies were used: anti–rabbit IgG (Cell Signaling Technology), anti-H3K4me3 (Active Motive), and anti-H3 (Abcam), as well as anti-H3ac, anit-H4ac, anti-H3K4me2, and anti-H3K9ac (all from Millipore).

Histology. Femurs and spleens were fixed in 10% formalin, femurs were subsequently decalcified in 10% buffered EDTA, pH 7.2, and all organs were paraffin embedded. Sections were stained with hematoxylin and eosin (H&E) for histological analysis, with Prussian blue for iron deposits, and with Gomori's silver stain to detect reticulin fibers, as well as with the Elastica van Gieson stain to detect vascularity.

Vorinostat treatment. NF-E2 tg and WT littermates were injected i.p. with 100 µg/g body weight vorinostat (SAHA; Selleck Chemicals) for a period of 11 d. SAHA was dissolved in DMSO and i.p. injected with a total volume of 100 µl in sunflower oil.

Data analysis. The Student's *t* test or the Mann-Whitney *U* test (Wilcoxon rank-sum test) was used, as appropriate, to determine whether a significant ($P < 0.05$) difference existed between two groups. When comparing more than two groups, a Kruskal–Wallis one-way analysis of variance (ANOVA) on Ranks or a one-way ANOVA was used. The association of hNF-E2 expression with ANC was assessed using Spearman's correlation coefficient.

Online supplemental material. Fig. S1 shows array-CGH of BM from five hNF-E2 tg mice to a pool of WT mice at the age of 18 mo. Fig. S2 depicts the gating strategies used to delineate stem and progenitor populations. Online supplemental material is available at http://www.jem.org/cgi/content/full/jem.20110540/DC1.

We sincerely thank Prof. Dr. W. Schempp and C. Holder (Institute of Human Genetics) for performing the interphase FISH and T. Lowka (Institute of Pathology) for histopathological staining, as well as L. Vandré and J. Marx for histological analysis. We are indebted to Prof. Dr. M. Luebbert and Dr. N. Friedrichs for insightful comments on the manuscript and to Prof. Dr. J. Goldberg, Dr. I. Belitskaya-Lévy, and L. Price (New York University Langone Medical Center, New York, NY), as well as to Prof. Dr. D.S. Neuberg and Dr. K. Stevenson (Dana-Farber Cancer Institute, Boston, MA) for statistical analysis. We sincerely thank Prof. Dr. D.G. Tenen and Dr. S. Koschmieder for the generous gift of the FVB/N 45.2 mice, and I. Pahl and Dr. F. Pahl for critical review of the manuscript.

This work was supported by grants from the National Cancer Institute (PO1 CA108671 to H.L. Pahl), the Deutsche Forschungsgemeinschaft (Pa 611/6-1 to H.L. Pahl), and the Roche Foundation for Anemia Research (to H.L. Pahl), as well as by a Seeding Grant from the Comprehensive Cancer Center Freiburg to K.B. Kaufmann. J.M. Wagner and M. Jung thank the Deutsche Forschungsgemeinschaft (Ju 295/9-1, SPP1463) for support. H.L. Pahl is a member of the Myeloproliferative Disorders Research Consortium. R. Bogeska was funded by the Excellence Initiative of the German Federal and States Governments (GSC-4, Spemann Graduate School).

The authors have no conflicting financial interests.

Submitted: 17 March 2011
Accepted: 2 December 2011

REFERENCES

Akada, H., D. Yan, H. Zou, S. Fiering, R.E. Hutchison, and M.G. Mohi. 2010. Conditional expression of heterozygous or homozygous Jak2V617F from its endogenous promoter induces a polycythemia vera-like disease. *Blood*. 115:3589–3597. http://dx.doi.org/10.1182/blood-2009-04-215848

Akashi, K., D. Traver, T. Miyamoto, and I.L. Weissman. 2000. A clonogenic common myeloid progenitor that gives rise to all myeloid lineages. *Nature*. 404:193–197. http://dx.doi.org/10.1038/35004599

Andrews, N.C., H. Erdjument-Bromage, M.B. Davidson, P. Tempst, and S.H. Orkin. 1993. Erythroid transcription factor NF-E2 is a haematopoietic-specific basic-leucine zipper protein. *Nature*. 362:722–728. http://dx.doi.org/10.1038/362722a0

Bench, A.J., E.P. Nacheva, K.M. Champion, and A.R. Green. 1998. Molecular genetics and cytogenetics of myeloproliferative disorders. *Baillieres Clin. Haematol*. 11:819–848. http://dx.doi.org/10.1016/S0950-3536(98)80041-3

Bilgrami, S., and B.R. Greenberg. 1995. Polycythemia rubra vera. *Semin. Oncol*. 22:307–326.

Bishton, M.J., S.J. Harrison, B.P. Martin, N. McLaughlin, C. James, E.C. Josefsson, K.J. Henley, B.T. Kile, H.M. Prince, and R.W. Johnstone. 2011. Deciphering the molecular and biologic processes that mediate histone deacetylase inhibitor-induced thrombocytopenia. *Blood*. 117:3658–3668. http://dx.doi.org/10.1182/blood-2010-11-318055

Boulanger, L., D.E. Sabatino, E.Y. Wong, A.P. Cline, L.J. Garrett, M. Garbarz, D. Dhermy, D.M. Bodine, and P.G. Gallagher. 2002. Erythroid expression of the human alpha-spectrin gene promoter is mediated by GATA-1- and NF-E2-binding proteins. *J. Biol. Chem*. 277:41563–41570. http://dx.doi.org/10.1074/jbc.M208184200

Brand, M., J.A. Ranish, N.T. Kummer, J. Hamilton, K. Igarashi, C. Francastel, T.H. Chi, G.R. Crabtree, R. Aebersold, and M. Groudine. 2004. Dynamic changes in transcription factor complexes during erythroid differentiation revealed by quantitative proteomics. *Nat. Struct. Mol. Biol*. 11:73–80. http://dx.doi.org/10.1038/nsmb713

Bulger, M., T. Sawado, D. Schübeler, and M. Groudine. 2002. ChIPs of the beta-globin locus: unraveling gene regulation within an active domain. *Curr. Opin. Genet. Dev*. 12:170–177. http://dx.doi.org/10.1016/S0959-437X(02)00283-6

Campbell, P.J., E.J. Baxter, P.A. Beer, L.M. Scott, A.J. Bench, B.J. Huntly, W.N. Erber, R. Kusec, T.S. Larsen, S. Giraudier, et al. 2006. Mutation of JAK2 in the myeloproliferative disorders: timing, clonality studies,

cytogenetic associations, and role in leukemic transformation. *Blood*. 108:3548–3555. http://dx.doi.org/10.1182/blood-2005-12-013748

Cario, H., P.S. Goerttler, C. Steimle, R.L. Levine, and H.L. Pahl. 2005. The JAK2V617F mutation is acquired secondary to the predisposing alteration in familial polycythaemia vera. *Br. J. Haematol*. 130:800–801. http://dx.doi.org/10.1111/j.1365-2141.2005.05683.x

Cervantes, F., F. Passamonti, and G. Barosi. 2008. Life expectancy and prognostic factors in the classic BCR/ABL-negative myeloproliferative disorders. *Leukemia*. 22:905–914. http://dx.doi.org/10.1038/leu.2008.72

Chaturvedi, C.P., A.M. Hosey, C. Palii, C. Perez-Iratxeta, Y. Nakatani, J.A. Ranish, F.J. Dilworth, and M. Brand. 2009. Dual role for the methyltransferase G9a in the maintenance of beta-globin gene transcription in adult erythroid cells. *Proc. Natl. Acad. Sci. USA*. 106:18303–18308. http://dx.doi.org/10.1073/pnas.0906769106

Chen, Z., M. Hu, and R.A. Shivdasani. 2007. Expression analysis of primary mouse megakaryocyte differentiation and its application in identifying stage-specific molecular markers and a novel transcriptional target of NF-E2. *Blood*. 109:1451–1459. http://dx.doi.org/10.1182/blood-2006-08-038901

Christensen, J.L., and I.L. Weissman. 2001. Flk-2 is a marker in hematopoietic stem cell differentiation: a simple method to isolate long-term stem cells. *Proc. Natl. Acad. Sci. USA*. 98:14541–14546. http://dx.doi.org/10.1073/pnas.261562798

Demers, C., C.P. Chaturvedi, J.A. Ranish, G. Juban, P. Lai, F. Morle, R. Aebersold, F.J. Dilworth, M. Groudine, and M. Brand. 2007. Activator-mediated recruitment of the MLL2 methyltransferase complex to the beta-globin locus. *Mol. Cell*. 27:573–584. http://dx.doi.org/10.1016/j.molcel.2007.06.022

Goerttler, P.S., C. Kreutz, J. Donauer, D. Faller, T. Maiwald, E. März, B. Rumberger, T. Sparna, A. Schmitt-Gräff, J. Wilpert, et al. 2005. Gene expression profiling in polycythaemia vera: overexpression of transcription factor NF-E2. *Br. J. Haematol*. 129:138–150. http://dx.doi.org/10.1111/j.1365-2141.2005.05416.x

Groupe Français de Cytogénétique Hématologique. 1988. Cytogenetics of acutely transformed chronic myeloproliferative syndromes without a Philadelphia chromosome. A multicenter study of 55 patients. *Cancer Genet. Cytogenet*. 32:157–168. http://dx.doi.org/10.1016/0165-4608(88)90278-6

Guibal, F.C., M. Alberich-Jorda, H. Hirai, A. Ebralidze, E. Levantini, A. Di Ruscio, P. Zhang, B.A. Santana-Lemos, D. Neuberg, A.J. Wagers, et al. 2009. Identification of a myeloid committed progenitor as the cancer-initiating cell in acute promyelocytic leukemia. *Blood*. 114:5415–5425. http://dx.doi.org/10.1182/blood-2008-10-182071

Huntly, B.J., H. Shigematsu, K. Deguchi, B.H. Lee, S. Mizuno, N. Duclos, R. Rowan, S. Amaral, D. Curley, I.R. Williams, et al. 2004. MOZ-TIF2, but not BCR-ABL, confers properties of leukemic stem cells to committed murine hematopoietic progenitors. *Cancer Cell*. 6:587–596. http://dx.doi.org/10.1016/j.ccr.2004.10.015

Hussein, K., D.L. Van Dyke, and A. Tefferi. 2009. Conventional cytogenetics in myelofibrosis: literature review and discussion. *Eur. J. Haematol*. 82:329–338. http://dx.doi.org/10.1111/j.1600-0609.2009.01224.x

Jamieson, C.H., J. Gotlib, J.A. Durocher, M.P. Chao, M.R. Mariappan, M. Lay, C. Jones, J.L. Zehnder, S.L. Lilleberg, and I.L. Weissman. 2006. The JAK2 V617F mutation occurs in hematopoietic stem cells in polycythemia vera and predisposes toward erythroid differentiation. *Proc. Natl. Acad. Sci. USA*. 103:6224–6229. http://dx.doi.org/10.1073/pnas.0601462103

Jones, A.V., A. Chase, R.T. Silver, D. Oscier, K. Zoi, Y.L. Wang, H. Cario, H.L. Pahl, A. Collins, A. Reiter, et al. 2009. JAK2 haplotype is a major risk factor for the development of myeloproliferative neoplasms. *Nat. Genet*. 41:446–449. http://dx.doi.org/10.1038/ng.334

Josefsson, E.C., C. James, K.J. Henley, M.A. Debrincat, K.L. Rogers, M.R. Dowling, M.J. White, E.A. Kruse, R.M. Lane, S. Ellis, et al. 2011. Megakaryocytes possess a functional intrinsic apoptosis pathway that must be restrained to survive and produce platelets. *J. Exp. Med*. 208:2017–2031. http://dx.doi.org/10.1084/jem.20110750

Kiekhaefer, C.M., J.A. Grass, K.D. Johnson, M.E. Boyer, and E.H. Bresnick. 2002. Hematopoietic-specific activators establish an overlapping pattern of histone acetylation and methylation within a mammalian chromatin domain. *Proc. Natl. Acad. Sci. USA*. 99:14309–14314. http://dx.doi.org/10.1073/pnas.212389499

Kiel, M.J., O.H. Yilmaz, T. Iwashita, O.H. Yilmaz, C. Terhorst, and S.J. Morrison. 2005. SLAM family receptors distinguish hematopoietic stem and progenitor cells and reveal endothelial niches for stem cells. *Cell*. 121:1109–1121. http://dx.doi.org/10.1016/j.cell.2005.05.026

Kogan, S.C., J.M. Ward, M.R. Anver, J.J. Berman, C. Brayton, R.D. Cardiff, J.S. Carter, S. de Coronado, J.R. Downing, T.N. Fredrickson, et al; Hematopathology subcommittee of the Mouse Models of Human Cancers Consortium. 2002. Bethesda proposals for classification of nonlymphoid hematopoietic neoplasms in mice. *Blood*. 100:238–245. http://dx.doi.org/10.1182/blood.V100.1.238

Koh, Y., I. Kim, J.Y. Bae, E.Y. Song, H.K. Kim, S.S. Yoon, D.S. Lee, S.S. Park, M.H. Park, S. Park, and B.K. Kim. 2010. Prognosis of secondary acute myeloid leukemia is affected by the type of the preceding hematologic disorders and the presence of trisomy 8. *Jpn. J. Clin. Oncol*. 40:1037–1045. http://dx.doi.org/10.1093/jjco/hyq097

Kralovics, R., S.S. Teo, S. Li, A. Theocharides, A.S. Buser, A. Tichelli, and R.C. Skoda. 2006. Acquisition of the V617F mutation of JAK2 is a late genetic event in a subset of patients with myeloproliferative disorders. *Blood*. 108:1377–1380. http://dx.doi.org/10.1182/blood-2005-11-009605

Lacout, C., D.F. Pisani, M. Tulliez, F.M. Gachelin, W. Vainchenker, and J.L. Villeval. 2006. JAK2V617F expression in murine hematopoietic cells leads to MPD mimicking human PV with secondary myelofibrosis. *Blood*. 108:1652–1660. http://dx.doi.org/10.1182/blood-2006-02-002030

Li, C.-Y. 2002. The role of morphology, cytochemistry and immunohistochemistry in the diagnosis of chronic myeloproliferative diseases. *Int. J. Hematol*. 76:6–8. http://dx.doi.org/10.1007/BF03165077

Li, J., D. Spensberger, J.S. Ahn, S. Anand, P.A. Beer, C. Ghevaert, E. Chen, A. Forrai, L.M. Scott, R. Ferreira, et al. 2010. JAK2 V617F impairs hematopoietic stem cell function in a conditional knock-in mouse model of JAK2 V617F-positive essential thrombocythemia. *Blood*. 116:1528–1538. http://dx.doi.org/10.1182/blood-2009-12-259747

Lu, S.J., S. Rowan, M.R. Bani, and Y. Ben-David. 1994. Retroviral integration within the Fli-2 locus results in inactivation of the erythroid transcription factor NF-E2 in Friend erythroleukemias: evidence that NF-E2 is essential for globin expression. *Proc. Natl. Acad. Sci. USA*. 91:8398–8402. http://dx.doi.org/10.1073/pnas.91.18.8398

Lundberg, L.G., R. Lerner, P. Sundelin, R. Rogers, J. Folkman, and J. Palmblad. 2000. Bone marrow in polycythemia vera, chronic myelocytic leukemia, and myelofibrosis has an increased vascularity. *Am. J. Pathol*. 157:15–19. http://dx.doi.org/10.1016/S0002-9440(10)64511-7

Majeti, R., C.Y. Park, and I.L. Weissman. 2007. Identification of a hierarchy of multipotent hematopoietic progenitors in human cord blood. *Cell Stem Cell*. 1:635–645. http://dx.doi.org/10.1016/j.stem.2007.10.001

Matsuoka, H., A. Unami, T. Fujimura, T. Noto, Y. Takata, K. Yoshizawa, H. Mori, I. Aramori, and S. Mutoh. 2007. Mechanisms of HDAC inhibitor-induced thrombocytopenia. *Eur. J. Pharmacol*. 571:88–96. http://dx.doi.org/10.1016/j.ejphar.2007.06.015

Moroni, E., T. Mastrangelo, R. Razzini, L. Cairns, P. Moi, S. Ottolenghi, and B. Giglioni. 2000. Regulation of mouse p45 NF-E2 transcription by an erythroid-specific GATA-dependent intronic alternative promoter. *J. Biol. Chem*. 275:10567–10576. http://dx.doi.org/10.1074/jbc.275.14.10567

Mutschler, M., A.S. Magin, M. Buerge, R. Roelz, D.H. Schanne, B. Will, I.H. Pilz, A.R. Migliaccio, and H.L. Pahl. 2009. NF-E2 overexpression delays erythroid maturation and increases erythrocyte production. *Br. J. Haematol*. 146:203–217. http://dx.doi.org/10.1111/j.1365-2141.2009.07742.x

Nussenzveig, R.H., S.I. Swierczek, J. Jelinek, A. Gaikwad, E. Liu, S. Verstovsek, J.F. Prchal, and J.T. Prchal. 2007. Polycythemia vera is not initiated by JAK2V617F mutation. *Exp. Hematol*. 35:32–38. http://dx.doi.org/10.1016/j.exphem.2006.11.012

Ogilvy, S., D. Metcalf, L. Gibson, M.L. Bath, A.W. Harris, and J.M. Adams. 1999. Promoter elements of vav drive transgene expression in vivo throughout the hematopoietic compartment. *Blood*. 94:1855–1863.

Onishi, Y., and R. Kiyama. 2003. Interaction of NF-E2 in the human beta-globin locus control region before chromatin remodeling. *J. Biol. Chem*. 278:8163–8171. http://dx.doi.org/10.1074/jbc.M209612200

Orlic, D., S. Anderson, L.G. Biesecker, B.P. Sorrentino, and D.M. Bodine. 1995. Pluripotent hematopoietic stem cells contain high levels of mRNA for c-kit, GATA-2, p45 NF-E2, and c-myb and low levels or no mRNA for c-fms and the receptors for granulocyte colony-stimulating factor and interleukins 5 and 7. *Proc. Natl. Acad. Sci. USA*. 92:4601–4605. http://dx.doi.org/10.1073/pnas.92.10.4601

Passamonti, F., E. Rumi, E. Pungolino, L. Malabarba, P. Bertazzoni, M. Valentini, E. Orlandi, L. Arcaini, E. Brusamolino, C. Pascutto, et al. 2004. Life expectancy and prognostic factors for survival in patients with polycythemia vera and essential thrombocythemia. *Am. J. Med.* 117:755–761. http://dx.doi.org/10.1016/j.amjmed.2004.06.032

Passegué, E., C.H. Jamieson, L.E. Ailles, and I.L. Weissman. 2003. Normal and leukemic hematopoiesis: are leukemias a stem cell disorder or a reacquisition of stem cell characteristics? *Proc. Natl. Acad. Sci. USA*. 100:11842–11849. http://dx.doi.org/10.1073/pnas.2034201100

Passegué, E., A.J. Wagers, S. Giuriato, W.C. Anderson, and I.L. Weissman. 2005. Global analysis of proliferation and cell cycle gene expression in the regulation of hematopoietic stem and progenitor cell fates. *J. Exp. Med.* 202:1599–1611. http://dx.doi.org/10.1084/jem.20050967

Pikman, Y., B.H. Lee, T. Mercher, E. McDowell, B.L. Ebert, M. Gozo, A. Cuker, G. Wernig, S. Moore, I. Galinsky, et al. 2006. MPLW515L is a novel somatic activating mutation in myelofibrosis with myeloid metaplasia. *PLoS Med.* 3:e270. http://dx.doi.org/10.1371/journal.pmed.0030270

Prchal, J.F., and A.A. Axelrad. 1974. Letter: Bone-marrow responses in polycythemia vera. *N. Engl. J. Med.* 290:1382.

Pronk, C.J., D.J. Rossi, R. Månsson, J.L. Attema, G.L. Norddahl, C.K. Chan, M. Sigvardsson, I.L. Weissman, and D. Bryder. 2007. Elucidation of the phenotypic, functional, and molecular topography of a myeloerythroid progenitor cell hierarchy. *Cell Stem Cell*. 1:428–442. http://dx.doi.org/10.1016/j.stem.2007.07.005

Rambaldi, A., C.M. Dellacasa, G. Finazzi, A. Carobbio, M.L. Ferrari, P. Guglielmelli, E. Gattoni, S. Salmoiraghi, M.C. Finazzi, S. Di Tollo, et al. 2010. A pilot study of the Histone-Deacetylase inhibitor Givinostat in patients with JAK2V617F positive chronic myeloproliferative neoplasms. *Br. J. Haematol.* 150:446–455.

Ried, T., A. Baldini, T.C. Rand, and D.C. Ward. 1992. Simultaneous visualization of seven different DNA probes by in situ hybridization using combinatorial fluorescence and digital imaging microscopy. *Proc. Natl. Acad. Sci. USA*. 89:1388–1392. http://dx.doi.org/10.1073/pnas.89.4.1388

Santos, F.P., H.M. Kantarjian, N. Jain, T. Manshouri, D.A. Thomas, G. Garcia-Manero, D. Kennedy, Z. Estrov, J. Cortes, and S. Verstovsek. 2010. Phase 2 study of CEP-701, an orally available JAK2 inhibitor, in patients with primary or post-polycythemia vera/essential thrombocythemia myelofibrosis. *Blood*. 115:1131–1136. http://dx.doi.org/10.1182/blood-2009-10-246363

Schempp, W., A. Binkele, J. Arnemann, B. Gläser, K. Ma, K. Taylor, R. Toder, J. Wolfe, S. Zeitler, and A.C. Chandley. 1995. Comparative mapping of YRRM- and TSPY-related cosmids in man and hominoid apes. *Chromosome Res.* 3:227–234. http://dx.doi.org/10.1007/BF00713047

Shi, J., Y. Zhao, T. Ishii, W. Hu, S. Sozer, W. Zhang, E. Bruno, V. Lindgren, M. Xu, and R. Hoffman. 2007. Effects of chromatin-modifying agents on CD34+ cells from patients with idiopathic myelofibrosis. *Cancer Res.* 67:6417–6424. http://dx.doi.org/10.1158/0008-5472.CAN-07-0572

Silva, M., C. Richard, A. Benito, C. Sanz, I. Olalla, and J.L. Fernández-Luna. 1998. Expression of Bcl-x in erythroid precursors from patients with polycythemia vera. *N. Engl. J. Med.* 338:564–571. http://dx.doi.org/10.1056/NEJM199802263380902

Steinemann, D., G. Cario, M. Stanulla, L. Karawajew, M. Tauscher, A. Weigmann, G. Göhring, W.D. Ludwig, J. Harbott, B. Radlwimmer, et al. 2008. Copy number alterations in childhood acute lymphoblastic leukemia and their association with minimal residual disease. *Genes Chromosomes Cancer*. 47:471–480. http://dx.doi.org/10.1002/gcc.20557

Steiner, L.A., Y. Maksimova, V. Schulz, C. Wong, D. Raha, M.C. Mahajan, S.M. Weissman, and P.G. Gallagher. 2009. Chromatin architecture and transcription factor binding regulate expression of erythrocyte membrane protein genes. *Mol. Cell. Biol.* 29:5399–5412. http://dx.doi.org/10.1128/MCB.00777-09

Swerdlow, S., E. Campo, and N.L. Harris, E.S. Jaffe, S.A. Pileri, H. Stein, J. Thiele, and J.W. Vardiman. 2008. WHO Classification of Tumours of Haematopoietic and Lymphoid Tissues. Fourth edition. IRAC Press, Lyon, France. 441 pp.

Theocharides, A., M. Boissinot, F. Girodon, R. Garand, S.S. Teo, E. Lippert, P. Talmant, A. Tichelli, S. Hermouet, and R.C. Skoda. 2007. Leukemic blasts in transformed JAK2-V617F-positive myeloproliferative disorders are frequently negative for the JAK2-V617F mutation. *Blood*. 110:375–379. http://dx.doi.org/10.1182/blood-2006-12-062125

Tiwari, S., J.E. Italiano Jr., D.C. Barral, E.H. Mules, E.K. Novak, R.T. Swank, M.C. Seabra, and R.A. Shivdasani. 2003. A role for Rab27b in NF-E2-dependent pathways of platelet formation. *Blood*. 102:3970–3979. http://dx.doi.org/10.1182/blood-2003-03-0977

Toki, T., K. Arai, K. Terui, N. Komatsu, M. Yokoyama, F. Katsuoka, M. Yamamoto, and E. Ito. 2000. Functional characterization of the two alternative promoters of human p45 NF-E2 gene. *Exp. Hematol.* 28:1113–1119. http://dx.doi.org/10.1016/S0301-472X(00)00523-3

van der Holt, B., D.A. Breems, H. Berna Beverloo, E. van den Berg, A.K. Burnett, P. Sonneveld, and B. Löwenberg. 2007. Various distinctive cytogenetic abnormalities in patients with acute myeloid leukaemia aged 60 years and older express adverse prognostic value: results from a prospective clinical trial. *Br. J. Haematol.* 136:96–105. http://dx.doi.org/10.1111/j.1365-2141.2006.06403.x

Verstovsek, S., H. Kantarjian, R.A. Mesa, A.D. Pardanani, J. Cortes-Franco, D.A. Thomas, Z. Estrov, J.S. Fridman, E.C. Bradley, S. Erickson-Viitanen, et al. 2010. Safety and efficacy of INCB018424, a JAK1 and JAK2 inhibitor, in myelofibrosis. *N. Engl. J. Med.* 363:1117–1127. http://dx.doi.org/10.1056/NEJMoa1002028

Wang, J.C., C. Chen, T. Dumlao, S. Naik, T. Chang, Y.Y. Xiao, I. Sominsky, and J. Burton. 2008. Enhanced histone deacetylase enzyme activity in primary myelofibrosis. *Leuk. Lymphoma*. 49:2321–2327. http://dx.doi.org/10.1080/10428190802527699

Wang, W., S. Schwemmers, E.O. Hexner, and H.L. Pahl. 2010a. AML1 is overexpressed in patients with myeloproliferative neoplasms and mediates JAK2V617F-independent overexpression of NF-E2. *Blood*. 116:254–266. http://dx.doi.org/10.1182/blood-2009-11-254664

Wang, X., W. Zhang, T. Ishii, S. Sozer, J. Wang, M. Xu, and R. Hoffman. 2009. Correction of the abnormal trafficking of primary myelofibrosis CD34+ cells by treatment with chromatin-modifying agents. *Cancer Res.* 69:7612–7618. http://dx.doi.org/10.1158/0008-5472.CAN-09-1823

Wang, X., W. Zhang, J. Tripodi, M. Lu, M. Xu, V. Najfeld, Y. Li, and R. Hoffman. 2010b. Sequential treatment of CD34+ cells from patients with primary myelofibrosis with chromatin-modifying agents eliminate JAK2V617F-positive NOD/SCID marrow repopulating cells. *Blood*. 116:5972–5982. http://dx.doi.org/10.1182/blood-2010-02-269696

Wehmeier, A., I. Daum, H. Jamin, and W. Schneider. 1991. Incidence and clinical risk factors for bleeding and thrombotic complications in myeloproliferative disorders. A retrospective analysis of 260 patients. *Ann. Hematol.* 63:101–106. http://dx.doi.org/10.1007/BF01707281

Wernig, G., T. Mercher, R. Okabe, R.L. Levine, B.H. Lee, and D.G. Gilliland. 2006. Expression of Jak2V617F causes a polycythemia vera-like disease with associated myelofibrosis in a murine bone marrow transplant model. *Blood*. 107:4274–4281. http://dx.doi.org/10.1182/blood-2005-12-4824

Will, B., and U. Steidl. 2010. Multi-parameter fluorescence-activated cell sorting and analysis of stem and progenitor cells in myeloid malignancies. *Best Pract. Res. Clin. Haematol.* 23:391–401. http://dx.doi.org/10.1016/j.beha.2010.06.006

Zhang, Y., K. Chen, Y. Tu, and C. Wu. 2004. Distinct roles of two structurally closely related focal adhesion proteins, alpha-parvins and beta-parvins, in regulation of cell morphology and survival. *J. Biol. Chem.* 279:41695–41705. http://dx.doi.org/10.1074/jbc.M401563200